Stochastic energetics of non-linear oscillators in active baths

A Thesis

submitted to

Indian Institute of Science Education and Research Pune
in partial fulfillment of the requirements for the
BS-MS Dual Degree Programme

by

Ashwin Gopal

Indian Institute of Science Education and Research Pune
Dr. Homi Bhabha Road,
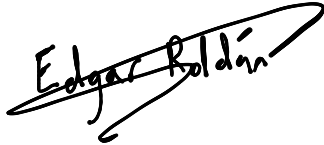Pashan, Pune 411008, INDIA.

April, 2020

Supervisor: Prof. Édgar Roldán , Co-supervisor: Prof. Stefano Ruffo
ⓒ Ashwin Gopal   2020

Certificate

This is to certify that this dissertation entitled *Stochastic energetics of non-linear oscillators in active baths* towards the partial fulfilment of the BS-MS dual degree programme at the Indian Institute of Science Education and Research, Pune, represents study/work carried out by Ashwin Gopal at the Abdus Salam International Centre for Theoretical Physics(ICTP), Trieste and Scuola Internazionale Superiore di Studi Avanzati(SISSA),Trieste under the supervision of Prof. Édgar Roldán and Prof. Stefano Ruffo, during the academic year 2019-2020.

Prof. Édgar Roldán   Ashwin Gopal

Committee:

    Prof. Édgar Roldán , Prof. Stefano Ruffo

    Prof. Deepak Dhar

This thesis is dedicated to Amma, Appa, Anu & all those affected by COVID-19

Declaration

I hereby declare that the matter embodied in the report entitled *Stochastic energetics of non-linear oscillators in active baths* , is the result of the work carried out by me, as a part of the BS-MS dual degree programme at the Indian Institute of Science Education and Research, Pune, at the Abdus Salam International Centre for Theoretical Physics(ICTP), Trieste and Scuola Internazionale Superiore di Studi Avanzati(SISSA),Trieste, under the supervision of Prof. Édgar Roldán and Prof. Stefano Ruffo and the same has not been submitted elsewhere for any other degree.

Prof. Édgar Roldán   Ashwin Gopal

Acknowledgment

I would like to first acknowledge the supervisors,Prof. Édgar Roldán and Prof. Stefano Ruffo, for providing their valuable scientific inputs and motivation, in guiding me and the thesis in the right direction. I would also like to thank them for providing opportunities to attend schools, conferences and give seminars at different universities. This entire collaboration wouldn't have been possible without the support of the Abdus Salam International Centre for Theoretical Physics(ICTP), a golden example of scientific outreach to the developing world, and Scuola Internazionale Superiore di Studi Avanzati(SISSA). I would like to thank all the administrative staff of both these institutes for their quick and timely support regarding any bureaucratic issues.

During this thesis, I was part of Quantitative Life Science(QLS), ICTP and Statistical Physics department, SISSA. I am truly grateful to meet a lot of wonderful intellectual people during my stay. First of all, I would like to all the members of QLS section of ICTP, especially the ping-pong comrades ,Jacopo Grilli and Andrea Mazzaloni, who made me feel part of the community and added color to different aspects of my stay. I would also like to thank the members of Soft Matter Journal Club of ICTP, for organizing frequent meetings with interesting discussions and giving me the opportunity to present a scientific article. I would also like to thank my dear friend Odilon Duranthon, who made me realize my love for cooking.

The valuable discussions with Prof. J. Parrondo, Prof. Massimiliano Esposito, Matteo Polettini, Yuzuru Sato, Ivan Di Terlizzi, Sarah AM Loos, Étienne Fodor, Nenad Pavin, Iva Tolić, Rita Majumdar and Jacopo Grilli, helped me gain valuable insights about my study and exposed me to wide variety of interesting problems.

I would especially like to specially thank the expert examiner for this thesis, Prof. Deepak Dhar, who is also my academic mentor, for growing the seed of interest in Statistical Physics in me and also helping me develop good scientific practices. I also take this opportunity to thank all the faculty members of Indian Institute of Science Education and Research(IISER),

Pune, who had taken their valuable time to discuss and teach the fundamental courses. Life would have been less spicier without the fellow first floor members of Hostel-1 at IISER and I would like to thank all the fellow party members of Dota 2, who have been part and parcel of my college life. .

Last but not the least I am indebted to all my family members, especially, Amma, Appa, my sister Anagha and my brother-in-law Easwar for their constant support.

Abstract

Active matter are systems whose individual units continuously extract energy from the environment to do produce some mechanical output. Examples ranges from bacterial propulsion, Janus particles to flocks of birds. Non-equilibrium properties of active matter have been recently utilized to produce useful work and design systems to rectify the activity of the bath, yet little is known about the work extraction from an active medium. In this thesis, we carefully study the statistics of thermodynamic quantities of a non-linear oscillator, called Adler oscillator, kept in presence of an active bath(Eg. bacterial bath), in particular we compute the power and work inputted into the system. In the process, we also look at the case of thermal bath, which occurs as low-correlation time limit of the active bath and elaborate the effects of correlation time(activity) τ.In the presence of active bath, the effect of the correlation time has been explored for the overdamped system near the bifurcation point. The main results of the thesis are : (i) In the case of a thermal bath, we exactly derive analytical expressions for the average power and variance in work at large times inputted into the system in the overdamped limit.(ii) In the underdamped limit, we found that the system has very high relaxation time to reach a unique steady state in the bistable region,and hence one can see signs of hysteresis effects in the presence of bath for long computation times $O(10^7)$.(iii) Numerical studies have been done to show that unified colored noise approximation doesn't capture the steady state properties, whereas Fox's approximation converges for small correlation times until there isn't significant deviation from Gaussian distribution in the angular velocity. (iv)Control of the activity of the bath can be used to regulate the power statistics. (v) Increased activity of the bath can be used to enhance the diffusive behavior at the bifurcation point, more than in the thermal bath case. We also found that the variance in the work inputted at large times increases with the activity of the bath at the bifurcation point.(vi)Numerical studies suggest that for values above the bifurcation point, there exists a finite critical correlation time τ_c when the average power inputted into the system is minimum, that can be below the deterministic case.

Contents

Introduction

The goal of statistical mechanics is to explain the macroscopic changes in nature, in a probabilistic nature, with reduced macroscopic parameters, without keeping track of individual degrees of freedom. Equilibrium statistical mechanics provides a microscopic description for the empirical laws of thermodynamics. But in nature, most of the systems are out of equilibrium, either in the process of relaxation to equilibrium or others maintained out of equilibrium with a constant flux of energy. Active matter systems are examples of the latter case. There is also a rich phenomenology associated with non-linear system that are kept out of equilibrium, like spatio-temporal pattern formation in BZ reaction[1], self-organized criticality[2, 3] etc. In this thesis, we explore the role of fluctuations(both thermal and active) in the statistics of the thermodynamic quantities of a non-linear oscillator in a non-equilibrium steady state(NESS).
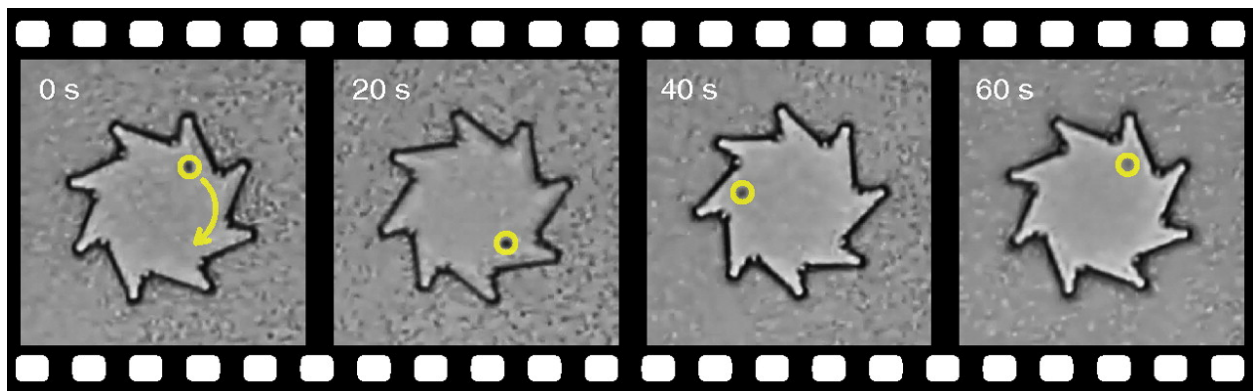

Figure 1: Micro-sized asymmetric rotor can be used to extract work from homogeneous medium of bacterial solution. Taken from [4]

Active Matter, systems with the individual particles continuously extracting energy from the different sources to produce some mechanical output, has recently attracted much of

1

attention in developing models in understanding their unique phenomenology and experiments to extract useful work. Examples of active matter range from biological systems to chemically processing systems, from motile sperm cells[5], bacterial colonies[6] to Janus particles[7]. These systems are inherently out of equilibrium, as they don't satisfy detailed balance, and show phenomenology which cannot be explained using equilibrium statistical mechanics. Some of the unique phenomenology includes motility-induced phase separation[8, 9, 10], even in the absence of attractive interactions (sometimes even with repulsive interactions), collective motion(flocking behaviour)[11], rectification phenomena[12, 4, 13] etc. Rectification phenomena, rectifying the activity of the system to produce work, has been successfully used to design micro-sized rotors to extract work from bacterial bath and also design spatial structures(with broken spatial symmetry) to produce unidirectional transport. Recent advances in optical tweezers, also led to the designing of highly efficient micro-sized heat engines in bacterial baths[14].
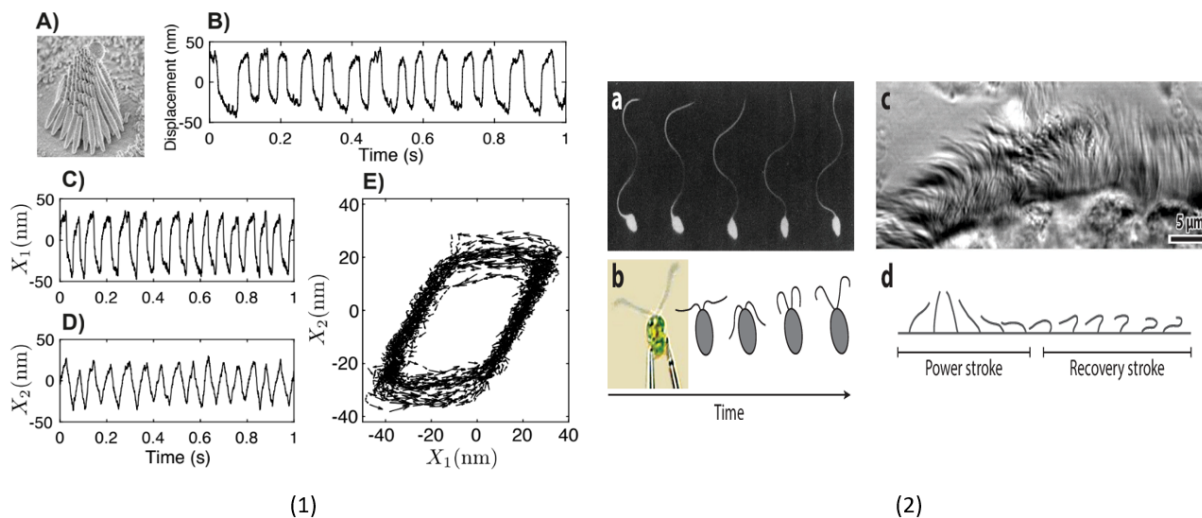

Figure 2: (1): Oscillatory Motion of the tip of hair bundle cells of Bullfrog, taken from [15], (2): Synchronization in cilia to help in cellular propulsion, taken from [16]

Non-linear dynamical systems are ubiquitous in nature and contribute to the complex structural and dynamical behaviour in nature. The dynamic nature of these systems is highly sensitive to the values of different parameters and initial conditions, which makes the study of such systems extremely interesting. Non-uniform oscillators are examples of such dynamical systems, where the instantaneous angular velocity is not constant. The dynamics

of non-uniform oscillator, similar to dynamics in a tilted periodic potential[17], has wide range applications in science and engineering. These are model systems used to study many physical systems like phase locked loops, superconducting Josephson tunneling junctions, motion of simple pendulum etc and biophysical processes like intra-cellular transport[18], spontaneous oscillations in mechanosensory hair bundle cells[19, 20] etc. One of an important application of such models is in understanding the phenomenon of synchronization[21],an emergent behaviour in the system of many coupled oscillators. Kuramoto model[22] is the "Ising model" of the analytical study of the dynamic transition of synchronization. Our model in interest, Adler model, corresponds to the mean field limit of the Kuramoto model.

Stochastic thermodynamics/energetics is a recent theoretical development, which extends the laws of macroscopic thermodynamics to mesoscopic scale, where fluctuations play an important role. The major advances in this field is in establishing successful correspondence of thermodynamic quantities to stochastic dynamics[23, 24, 25] and hence its application in understanding far from equilibrium systems. In addition to reproducing the macroscopic laws of thermodynamics, it extends these laws at the fluctuating level and one can deduce universal inequalities called fluctuation relations[26], which can be used to estimate equilibrium properties from a non-equilibrium protocols.
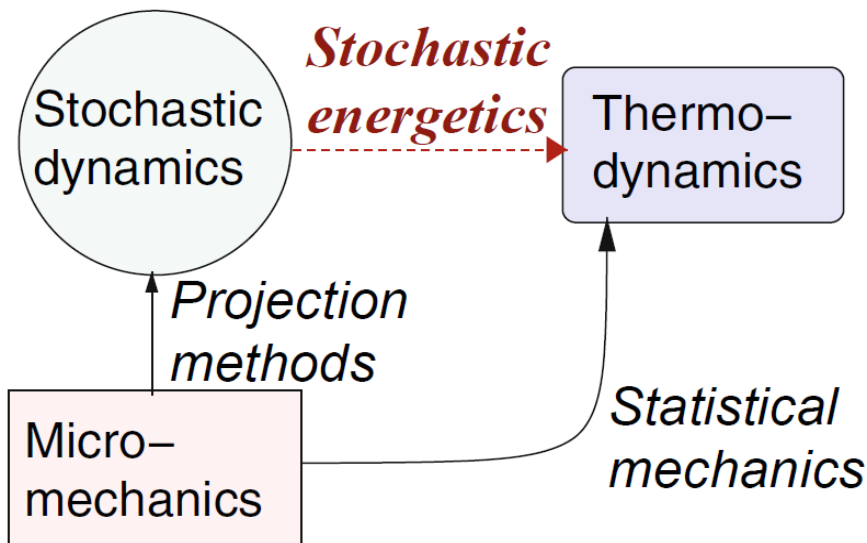

Figure 3: Stochastic Energetics/thermodynamics provides the missing link between stochastic dynamics and thermodynamics. Taken from [23].

The goal of this thesis was to understand the effect of fluctuations in the statistics of thermodynamic quantities for a non-linear system, near the bifurcation point. Active bath provides a great opportunity to study the role of non-equilibrium fluctuations in driving the system out of equilibrium. Non-linear oscillators, which are driven systems, already relaxes to non-equilibrium steady state in thermal bath. The role of active fluctuations in determining the deviations in steady state is to be evaluated and stochastic thermodynamics provides the tools needed to tackle the above questions.

In chapter 1, the preliminary theory and analytical tools developed in the thesis are discussed. A brief introduction to non-linear dynamical systems and stochastic thermodynamics is given. There is also section on the physics of active baths, where I review the literature on different approximations and also elucidate the thermodynamic formalism for such systems. In Chapter 2, I shift to our model of interest, the Adler oscillator. After a brief motivation for the model and its behaviour in deterministic limit, I explain the different results obtained for both overdamped and underdamped limit in the thermal bath. Finally, I explain the results obtained for the active bath case and compare it with the thermal bath for the overdamped case. In the last chapter, I briefly summarize the various results obtained through this study and will I outline our future directions.

Chapter 1

Preliminaries

This chapter will cover the basic analytical tools needed to understand the different results in this thesis.

1.1 Non-linear dynamical systems

In this section, I will review some of the basic dynamical features of non-linear systems under periodic boundary conditions in 1-D and 2-D[27]. In general, the n-dimensional equation of motion for a non-linear dynamical system is given by

$$\dot{x}_i = f_i(\vec{x} = \{x_i\}, \vec{r} = \{r_j\}) \tag{1.1}$$

where $f_i(x)$ can be non-linear function of instantaneous phase($\vec{x}$)of the system and $\vec{r}$ is the set of independent parameter such that $i \in \{1, 2.., n\}$ and $j \in \{1, 2.., m\}$.

Usually one is interested in the asymptotic behaviour of the dynamical system, i.e. dynamics as $t \to \infty$. The different asymptotic invariant structures depend on the form of $f_i(\{x_i\}, \{r_j\})$ and the dimension of the system. These invariant structures are given by solving $f_i(\{x_i\}, \{r_j\}) = 0$ and the stability of the different solutions depends on $\{r_j\}$. The stability of these invariant sets can be understood by linearizing the dynamics around these invariant solution(with a few exceptions)[27]. This method, called as linear stability analysis,

involves studying the properties of the Jacobian matrix $J(x)$, defined as,

$$J(\vec{x}) = \frac{\partial \vec{f}}{\partial \vec{x}} \tag{1.2}$$

where $\vec{f} = (\{f_i\})$.

If the real part of all the eigenvalues of the $J(\vec{x}^*)$ are negative, the invariant solution is stable. For a 1-d system, the only possible invariant solutions are fixed points, whereas in 2-d systems, in addition to fixed points, there are also limit cycles. The fixed points are further classified into nodes, spirals and centers based on the dynamic approach to the fixed point. Limit cycles are signatures of driven-dissipative physical systems(non-linear), are isolated closed orbits (different from periodic orbits which are not isolated). Based on the stability, the system either falls into or out of the limit cycle asymptotically. Stable limit cycles are found in many examples in nature, where the system has self-sustained oscillations, like rhythmic behaviour of heart beat, neuron firing, circadian rhythm. Small perturbation in these systems doesn't disrupt the properties of the oscillatory behaviour of such systems.

One defines bifurcation as a point in parameter space, where the stability of solutions change as one locally change the parameter values. Let us define invariant solutions, $x^*(\vec{r})$ as the solution of the equation $f_i(\{x_i\}, \{r_i\}) = 0$. One can then define bifurcation point(a point in the parameter space), The key aspect of such points is that different set of non-linear systems can categorized under the finite number of different bifurcations and, near the bifurcation point, these different systems have universal behaviour.

In 1-d systems, there are mainly three different kinds of bifurcations : Saddle-node bifurcation, Pitch-fork bifurcation(super- & sub-critical) and trans-critical bifurcation. Here, I will mainly describe the properties of the saddle-node bifurcation. The normal form (local behaviour near bifurcation point) for saddle-node bifurcation is given by

$$\dot{x} = r + x^2 \tag{1.3}$$

For such systems, for $r < 0$, it has both stable and unstable fixed point, which converges to become a saddle fixed point at $r = 0$ to no-stable solutions for $r > 0$. The presence of dynamical bottleneck is a signature of system near this bifurcation, and has square-root scaling law for the time taken to cross the bottleneck.

6

$$T_{bottleneck} \sim \int_{-\infty}^{\infty} dx \frac{1}{r + x^2} \propto \frac{1}{\sqrt{r}} \qquad (1.4)$$

The behaviour of a dynamical systems near bifurcation point have similarities to statistical behaviour near phase transition. The dynamic systems also follows power law(scaling) nature near bifurcation point as similar to the universal behaviour in phase transitions and different dynamical systems within the same bifurcation behaves similarly close to the bifurcation point. As explained above, near the saddle-node bifurcation, the system experiences a bottleneck, which is similar to the critical slow down. The key difference between phase transition in statistical physics and bifurcation in the dynamical system is that bifurcations occur for finite- dimensional systems whereas phase transition is defined at thermodynamic limit. But the bifurcation behaviour is related to the properties of asymptotic invariant solutions, which can be related to the idea of thermodynamic limit. One can also notice the similarities between the bifurcation diagram for super-critical pitchfork bifurcation(Fig.1.1) and the critical phase transition for magnetic systems with temperature. But the addition of bath(canonical ensemble) into a finite dimensional dynamical system, destroys the bifurcation behavior as fluctuations help explore the entire phase space even at the asymptotic limit, but effect of fluctuation near bifurcation point can have interesting applications as it can induce the system to have noise induced effects like noise-induced chaos, stochastic resonance wtc. as the system can explore topologically different solutions.

In 2d systems, in addition to the above mentioned bifurcations, one also has global bifurcations of the cycles- Hopf bifurcation, saddle-node bifurcation of cycles, infinite period bifurcation and homoclinic bifurcations. Hopf bifurcation is the most common among these bifurcations, which occurs when periodic orbit/limit cycles appears around a fixed point as one vary the parameter. Saddle-node bifurcation of cycles is similar to 1-D case, where stable and unstable limit cycles converge to become a saddle limit cycle at the bifurcation point. In infinite period bifurcation[See Fig.1.2(a)], nearby stable and unstable node converge to become a limit cycle above the bifurcation point. Finally, homoclinic bifurcation occurs when limit cycle whose size grows with parameter, gets destroyed when it meets a saddle node, through a homoclinic orbit. All of these bifurcations are mainly different from each other on the different scaling behaviour for time period and amplitude of oscillations with the dimensionless distance from the bifurcation point μ[See Fig.1.2(b)].
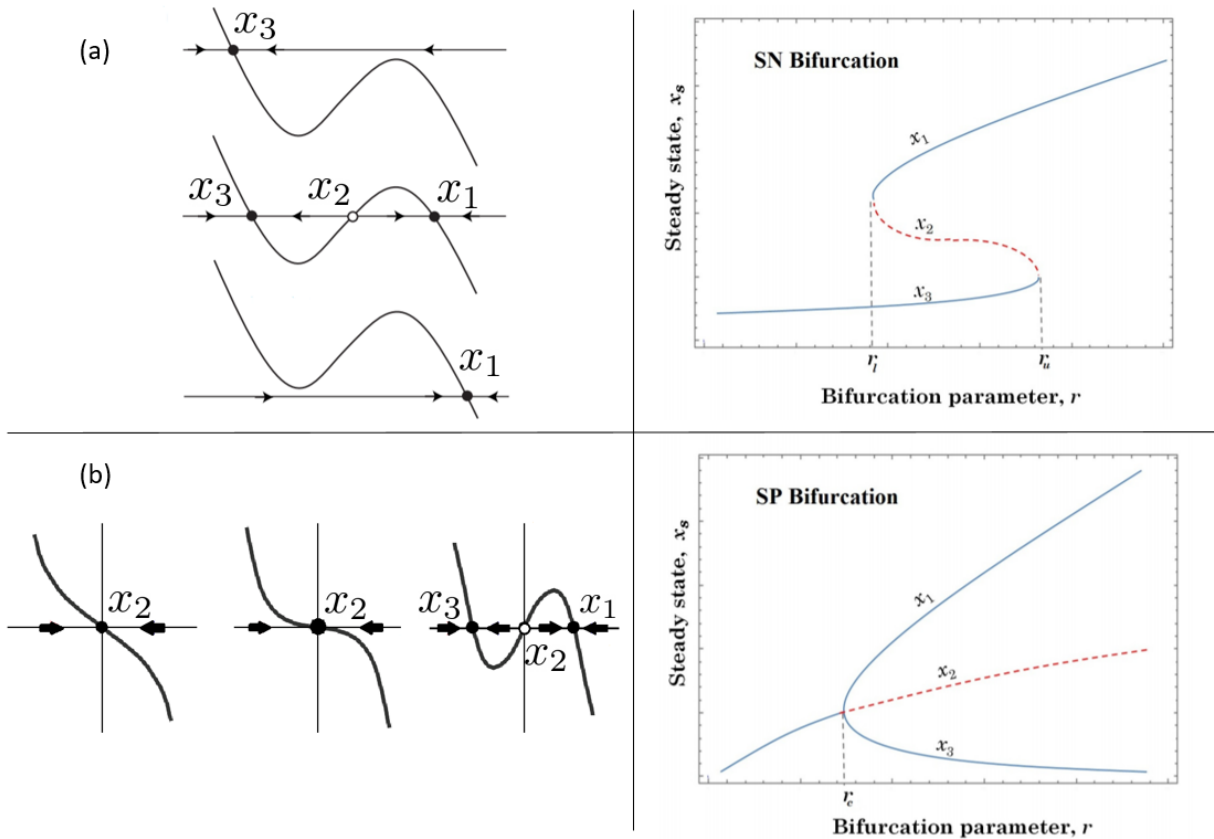
Figure 1.1: Examples of two kinds of bifurcations in 1-D dynamical system, where on the left is the plot of $\dot{x}$ vs x(flow diagram) and on the right is Bifurcation diagram plotting the asymptotic solutions for different parameter values : (a): Saddle-Node(SN) Bifurcation with Bistability between r_l and r_u, . (b): Supercritical Pitchfork(SP) Bifurcation. Adapted from [28]
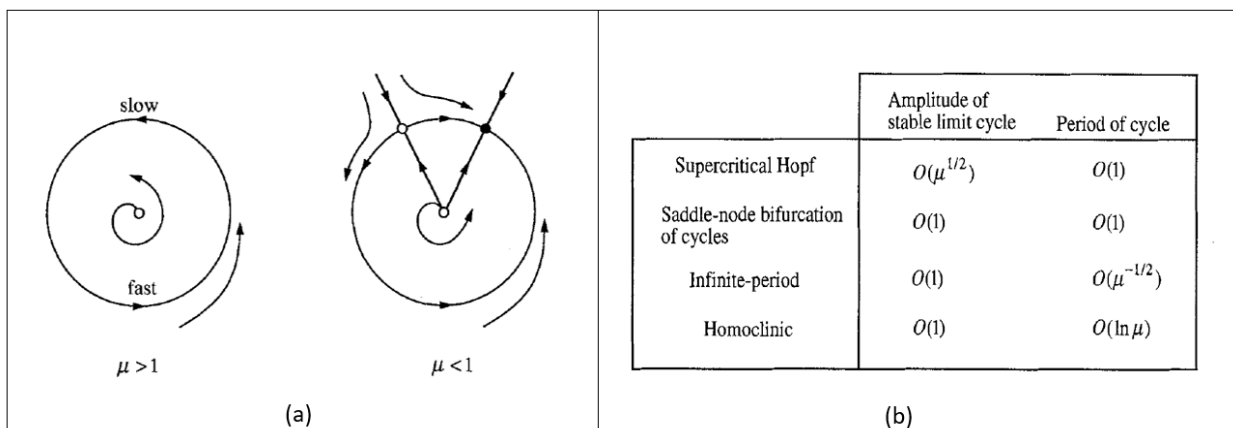

Figure 1.2: (a): Flow diagram for infinite period bifurcation for system where limit cycle(stable solution for $\mu > 1$) gets destroyed as we change μ, $\dot{x} = x(1 - x^2); \dot{y} = \mu - \sin y$. (b): The scaling behaviour of different global bifurcations related to limit cycles.

1.2 Stochastic Thermodynamics

The laws of thermodynamics are set of empirical laws which explain the macroscopic energy changes, even for system out of equilibrium. Even though equilibrium statistical mechanics provides a microscopic derivation for these laws, there exists no such universal theory to capture for out of equilibrium systems. The key step taken in this direction, was through linear irreversible thermodynamics, a semi-empirical theory combining the ideas of linear response theory to thermodynamic fluxes, which describes systems close to equilibrium. Stochastic thermodynamics, thermodynamic description for stochastic systems, extends even to systems far from equilibrium. It has been successfully used to describe the thermodynamic exchanges and expand the idea of irreversibility and dissipation for non-equilibrium systems in mesoscopic scale.
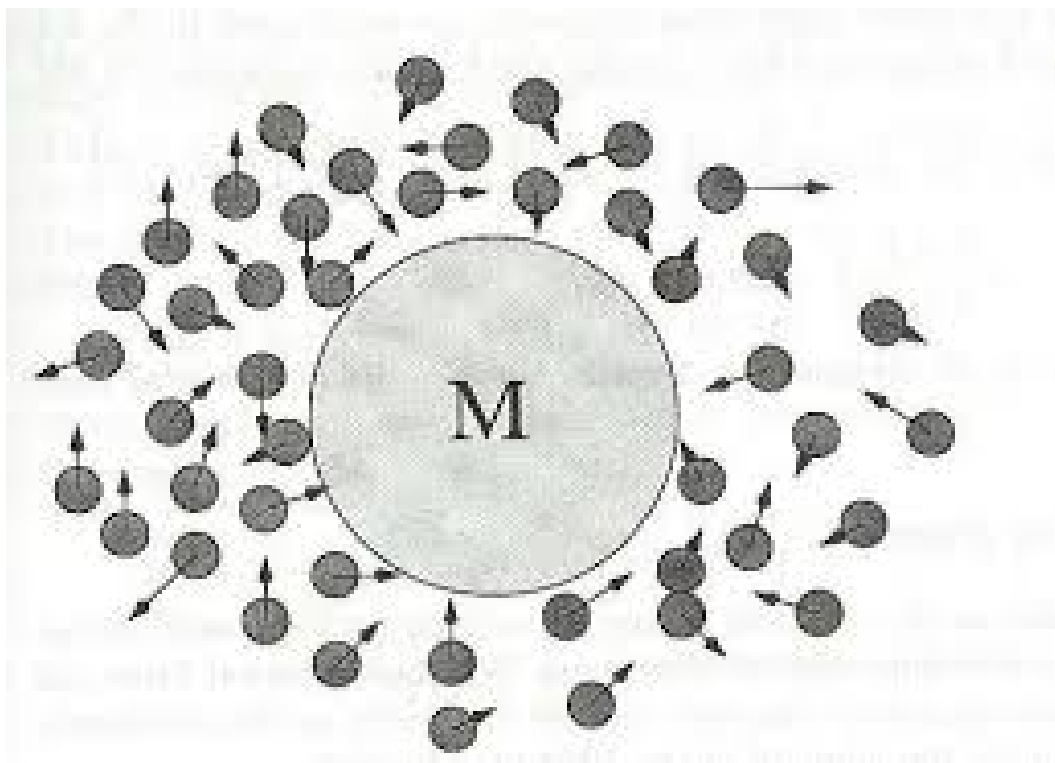
Figure 1.3: Motion of a colloidal particle of mass M under the effect of collisions from solvent molecules is well captured by Langevin dynamics. Taken from [29]

Langevin equation provides a coarse grained description of the motion of colloidal particle in a solvent. Such a coarse graining works reliably for systems where there is separation of time scales between the time-scale associated with motion of the colloidal particle and the

solvent particle. Consider, a colloidal particle of mass M, moving in solvent assumed to be a thermal bath of temperature,T, where the one-dimensional projection of the position is given by $x(t)$ at time t. Moreover, the motion of the colloidal particle is determined by time dependent conservative potential $\phi(x,t)$, with an external time dependent protocol and non-conservative force ,$F_{nc}(x,t)$ driving the system out of equilibrium. The coarse grained dynamics (Langevin dynamics) of the particles is given by

$$M\ddot{x}_t + \gamma\dot{x}_t = F_{nc}(x_t,t) - \phi'(x_t;t) + \eta_t \tag{1.5}$$

where $\phi'(x_t;t) = \frac{\partial\phi(x;t)}{\partial x}\Big|_{x=x_t}$ is the instantaneous force due to conservative potential and the effect of bath is captured in the two terms : $-\gamma\dot{x}$ relating the friction forces associated with the colloidal motion in the solvent and η_t is a random force term, the coarse grained force of many collision with the colloidal particle. In most cases, where the solvent particles are considered to be in equilibrium, the statistics of the random force are described by a Gaussian white noise with zero mean and auto-correlation function given by

$$\langle\eta_t\eta_{t'}\rangle = 2\gamma k_B T\delta(t - t') \tag{1.6}$$

where we have used the fact these noise follow fluctuation dissipation relation, i.e. strength of the noise $\sigma^2 = \langle\eta_t^2\rangle$ is given by $\sigma = \sqrt{2\gamma k_B T}$, where T is the temperature of the bath.

The thermodynamic quantities, then can be defined at the fluctuating trajectory level, following Sekimoto's definitions.The work done on the system on time interval ,$[t, t + dt]$, due to the forces controlled by an external agent, is given by

$$\delta W_t = \frac{\partial\phi(x_t;t)}{\partial t}dt + F_{nc}(x_t;t) \circ dx_t \tag{1.7}$$

$\circ$ corresponds to Stratonovich convention of stochastic calculus. Stratonovich convention is used as usual rules of calculus is applicable and first law of thermodynamics can be written in recognizable fashion[23].The infinitesimal heat inputted into the system is due to the forces associated with the thermal bath,and hence given by

$$\delta Q_t = (-\gamma\dot{x}_t + \eta_t) \circ dx_t = d\left[\frac{M\dot{x}_t^2}{2}\right] + \phi'_{\text{eff}}(x_t;t) \circ dx_t \tag{1.8}$$

where $\phi_{\text{eff}}(x;t) = \phi(x;t) - F_{nc}(x,t)x$ is the effective potential. The total energy of the system,

given by the sum of kinetic and potential energy,is given by

$$U(x_t, t) = \frac{M\dot{x}_t^2}{2} + \phi(x_t; t) \tag{1.9}$$

Hence the total work done and heat inputted into the system until time t along a trajectory, is given by,

$$Q(t) = \int_{x_o}^{x_t} (-\gamma\dot{x}_{t'} + \eta_{t'}) \circ dx_{t'} \tag{1.10}$$

$$W(t) = \int_0^t \frac{\partial\phi(x_t'; t')}{\partial t'} dt' + \int_{x_0}^{x_t} F_{nc}(x_t'; t') \circ dx_{t'} \tag{1.11}$$

One key observation is that both work and heat are not in general state function and dependent on the particular trajectory.

By simple rearrangement, one finds that first law of thermodynamics is obtained at the fluctuating trajectory level,

$$dU_t = \delta Q_t + \delta W_t \tag{1.12}$$

The idea of entropy was extended to non-equilibrium system, by using Shanon's definition of information, given by

$$\Delta S_{\text{sys}}(t) = k_B \ln \frac{P(x_t, \dot{x}_t; t)}{P(x_0, \dot{x}_0; 0)} \tag{1.13}$$

where $P(x_t, \dot{x}_t; t)$ is the phase space probability density and ΔS_{sys} is a state function, i.e. depends only on the initial and final states.

Now, assuming local detailed balance, one can define the entropy produced in the bath, as the log ratio of the conditional path probability of forwards trajectory to the conditional path probability of time reversed trajectory in a time reversed experiment, given as,

$$S_{\text{bath}}(t) = k_B \log \frac{P[\underline{x}_t, \underline{\dot{x}}_t | x_0, \dot{x}_0]}{\tilde{P}[\underline{\tilde{x}}_t, \underline{\tilde{\dot{x}}}_t | x_t, \dot{x}_t]} \tag{1.14}$$

where $\underline{x}_t = \{x(s)\}_{s=0}^{s=t}, \underline{\dot{x}}_t = \{\dot{x}\}_{s=0}^{s=t}$ corresponds to the trajectory in the phase space for the forward trajectory and $\tilde{x}_s = x_{t-s}, \tilde{\dot{x}}_s = -\dot{x}_{t-s}$ corresponds to time reversed point in phase space. The above definition of irreversibility(entropy production) can be related to

the dissipation in bath, by simple manipulations, as shown below,

$$\frac{P[\underline{x}_t, \underline{\dot{x}}_t | x_0, \dot{x}_0]}{\tilde{P}[\underline{\tilde{x}}_t, \underline{\tilde{\dot{x}}}_t | x_t, \dot{x}_t]} = \exp\left(\frac{-Q(t)}{k_B T}\right) \tag{1.15}$$

Hence the total entropy production is given by, $\Delta S_{tot} = \delta S_{bath} + \Delta S_{sys}$.

$$S_{\text{tot}}(t) = k_B \log \frac{P[\underline{x}_t, \underline{\dot{x}}_t]}{\tilde{P}[\underline{\tilde{x}}_t, \underline{\tilde{\dot{x}}}_t]} \tag{1.16}$$

One observes that the above definition of total entropy production fulfills, integral fluctuation relation, given by

$$\left\langle \exp\left[-\frac{S_{\text{tot}}}{k_B}\right] \right\rangle = 1 \tag{1.17}$$

from which we can use Jensen's inequality to obtain back the macroscopic 2nd law of thermodynamic, $\Delta S_{\text{tot}} \geq 0$, which is satisfied only in average. In stochastic thermodynamics, there can be trajectories where the total entropy production, but it can be shown that these are exponentially less likely compared to the positive counterpart, which scales with size of the system and hence, for a macroscopic system, $\Delta S_{\text{tot}} \geq 0$.

With the above framework, now we can define the steady state averages for the average power inputted into the system and average entropy production rate in the environment in the absence of time independent protocols and constant non-conservative forces.

$$\langle \dot{W} \rangle = \int P_s(x, \dot{x}) \dot{x} F_{nc} dx = \lim_{\mathcal{T} \to \infty} \frac{1}{\mathcal{T}} \int_0^{\mathcal{T}} F_{nc} \circ dx_t \tag{1.18}$$

$$\langle \sigma \rangle = -\left\langle \frac{\dot{Q}}{T} \right\rangle = \lim_{\mathcal{T} \to \infty} \frac{1}{\mathcal{T}} \left(\frac{M}{2} \left[\dot{x}_t^2 - \dot{x}_0^2\right] + \int_{x_0}^{x_{\mathcal{T}}} \phi'_{\text{eff}}(x_t) \circ dx_t \right) \tag{1.19}$$

where we have assumed ergodicity.

Recently, there has been growing interest in understanding the existence of fundamental trade-off between the precision and cost to keep a system in a non-equilibrium steady state, known as thermodynamic uncertainty relations (TURs). Currently there are many known such relations[30, 31, 32], which has been proven for Markovian systems in the steady state. Let J_t be the time-integrated current in the steady state till time t, then the finite time

TUR, is given by

$$\frac{\mathrm{Var}(\mathrm{J_t})}{\langle J_t \rangle^2} \geq \frac{2}{\langle \Delta S_{tot}(t) \rangle} \tag{1.20}$$

First passage properties have also been used to estimate the bounds for the entropy production in the steady state. Edgar *et.al*[31] showed that the lower bound for the steady state entropy production can be obtained using the mean first passage times for any suitable observable, x. Let us define, $\mathcal{T}(A) \equiv \inf\{\mathrm{t} \geq 0 / \mathrm{x(t)} \notin [\mathrm{x_{st}} - \mathrm{A}, \mathrm{x_{st}} + \mathrm{A}]\}$ where x_{st} is obtained from stationary distribution of the observable. The bound is given as,

$$\langle \dot{S_{\mathrm{tot}}} \rangle = \frac{D(A)}{\langle \mathcal{T}(A) \rangle} \tag{1.21}$$

where $\langle \mathcal{T}(A) \rangle$ is the mean first passage time to be absorbed in the any of the symmetric absorbing boundaries at $\pm A$ and $D(A)$ is the function of probability to be absorbed in one of the boundaries(error probability).

1.3 Physics of Active Bath

In this section, I will discuss the various analytical tools used to study the problem of Langevin dynamics in active bath and thermodynamic approach to the problem[33, 34]. Here, I will describe the coarse grained equation of motion for a colloidal particle in an active bath in the overdamped limit, i.e. time scale of observation is much more than the momentum relaxation time, is given by

$$\dot{x}_t = f(x_t) + \xi_t \tag{1.22}$$

such that the stochastic force is of the form of Gaussian distribution with zero mean and auto-correlation function given by

$$\langle \xi_t \xi_{t'} \rangle = \underbrace{\frac{D}{\tau} \exp\left(-\frac{|t - t'|}{\tau}\right)}_{\Gamma(t-t')} \tag{1.23}$$

where D is the strength of the noise and τ is the correlation time associated with the activity of the bath. This particular form is motivated by different experiments done on a colloidal tracer in bacterial bath[35, 36]. Since this noise doesn't satisfy fluctuation-dissipation

relation, it has features of an out-of-equilibrium system. This represents an example of non-Markovian Langevin equation of motion.Analytically, this problem is difficult to handle exactly for most forms of driving force, due to the non-Markovian nature in the 1-dimensional flow(Eqn(1.16)) or due to higher dimensional flow in Markovian regime (Eqn(1.26 − 27)).

The master equation corresponding to the above non-Markovian Langevin equation can be derived by using functional calculus methods. Solving the above SDE gives,

$$x_t = x_0 + \int_0^t ds \left[f(x_s) + \xi_s \right] \tag{1.24}$$

Now taking functional differentiation,

$$\frac{\delta x_t}{\delta \xi_{t'}} = 1 + \int_{t'}^t ds \left[f'(x_s) \right] \frac{\delta x_s}{\delta \xi_{t'}} \quad , \text{for t} > \text{t}' \tag{1.25}$$

$$\frac{\partial}{\partial t} \left(\frac{\delta x_t}{\delta \xi_{t'}} \right) = \left[f'(x_t) \right] \frac{\delta x_t}{\delta \xi_{t'}} \tag{1.26}$$

Solving the above differential equation, with initial condition $\frac{\delta x_{t'}}{\delta \xi_{t'}} = 1$. we get,

$$\frac{\delta x_t}{\delta \xi_{t'}} = \exp \left[\int_{t'}^t ds f'(x_s) \right] \tag{1.27}$$

One can map the above Langevin dynamics to a Master equation, to study the ensemble properties of the system. Defining, $P(x,t) = \langle \delta(x - x_t) \rangle$, where the average is over the realizations of noise and initial conditions. Using the properties of conservation of probability, one can derive the exact Master equation for $P(x,t)$[37],

$$\frac{\partial P(x,t)}{\partial t} = -\frac{\partial}{\partial x} \left[f(x) P(x,t) \right] - \frac{\partial}{\partial x} \left[\langle \xi_t \delta(x_t - x) \rangle \right] \tag{1.28}$$

Now the quantity which we need to evaluate and approximate is $\langle \xi_t \delta(x_t - x) \rangle$, for which we will use Novikov's theorem[Appendix A] and then using the properties of Dirac delta function, we get

$$\langle \xi_t \delta(x_t - x) \rangle = \int_0^t dt' \Gamma(t,t') \left\langle \frac{\delta[\delta(x_t - x)]}{\delta \xi_{t'}} \right\rangle \tag{1.29}$$

$$= -\int_0^t dt' \frac{\partial}{\partial x} \left[\frac{\delta x_t}{\delta \xi_{t'}} \bigg|_{x_t = x} \delta(x_t - x) \right] \Gamma(t,t') \tag{1.30}$$

Putting this back, we get,

$$\frac{\partial P(x,t)}{\partial t} = -\frac{\partial}{\partial x}\left[f(x)P(x,t)\right] + \frac{\partial}{\partial x}\left[\frac{\partial}{\partial x}\int_0^t dt'\Gamma(t,t')\left\langle \frac{\delta x_t}{\delta \xi_{t'}}\bigg|_{x_t=x}\delta(x_t-x)\right\rangle\right] \qquad (1.31)$$

We can see that for active bath case, the master equation doesn't not converge to Fokker Planck equation for general correlation time, τ. The non-Markovian behaviour is captured in the second term, as it cannot be written as single term of some higher order derivative of the instantaneous probability density. This term leads to infinite terms with higher order derivatives of instantaneous probability density if expanded in power series of correlation time.Below, we will show examples of some approximations which truncates the expansion at first order of expansion.

In many physical systems where the time scale separation is not sharp, the fluctuations in the equations of motion are modelled using "colored" noise, which introduces the effect of memory in the fluctuations, τ[34]. It is also commonly used to study the velocity dynamics of an active particle, like the motion of E.Coli., where τ is the persistence time of particle[38]. Here, we will use the model of Active Ornstein-Uhlenbeck dynamics, as it provides reasonable model for the motion of colloidal tracer in dense bacterial bath (not dense enough to give collective phenomena[38]). So, the effective Markovian dynamics in the extended space producing the above statistics is given by

$$\dot{x}_t \quad = f(x_t) + \xi_t \qquad (1.32)$$
$$\dot{\xi}_t \quad = -\frac{\xi_t}{\tau} + \frac{\sqrt{2D}}{\tau}\eta_t \qquad (1.33)$$

where η_t is Gaussian white noise with zero mean and unit variance.

The corresponding Fokker-Planck equation for the extended (x,ξ) space can be easily derived to be given by

$$\frac{\partial P}{\partial t}(x,\xi,t) = -\frac{\partial}{\partial x}\left[(f(x)+\xi)P\right] + \frac{\partial}{\partial \xi}\left[\left(\frac{\xi}{\tau}+\frac{D_0}{\tau^2}\frac{\partial}{\partial \xi}\right)P\right] \qquad (1.34)$$

Therefore, to obtain the stationary marginal distribution, we integrate out ξ, to obtain,

$$\rho(x)[f(x)+\bar{\xi}] = J_0 \qquad (1.35)$$

where $\rho(x) = \int d\xi P_s(x, \xi)$, $\bar{\xi} = \frac{1}{\rho(x)} \int \xi P_s(x, \xi) d\xi$ and where J_0 is the constant current in the steady state. The difficulty of handling such a equation analytically, is in computing $\bar{\xi}$, which requires the knowledge of the full density,$P_s(x, \xi)$.

Next, I will discuss some of the Markovian approximations used to convert the non-Markovian Master equation(Eqn.1.30) as as "Effective Fokker-Planck equation".

1. Sancho's approximation

This approximation[37] is a perturbation method based on truncation of the expansion of second term of master equation (Eqn. 1.30), upto first order in τ.In the vicinity of $t \to t'$,

$$\frac{\delta x_t}{\delta \xi_{t'}} \sim \left. \frac{\delta x_t}{\delta \xi_{t'}} \right|_{t=t'} + \left. \frac{d}{dt'} \frac{\delta x_t}{\delta \xi_{t'}} \right|_{t=t'} (t' - t) + O((t' - t)^2) \tag{1.36}$$

From Eqn. 1.26, we get,

$$\left. \frac{\delta x_t}{\delta \xi_{t'}} \right|_{t=t'} = 1, \quad \left. \frac{d}{dt'} \frac{\delta x_t}{\delta \xi_{t'}} \right|_{t=t'} = -f'(x_t) \tag{1.37}$$

Putting back everything together with correlation function defined by Eqn. (1.22), assuming $(t - t') \sim \tau$, we get,

$$\int_0^t dt' \Gamma(t, t') \left\langle \left. \frac{\delta x_t}{\delta \xi_{t'}} \right|_{x_t=x} \delta(x_t - x) \right\rangle = \int_0^t dt' \frac{\exp(-(t-t')/\tau)}{\tau} \langle (1 + \tau f'(x)) \delta(x_t - x) \rangle$$

$$= \int_0^t dt' D \frac{\exp(-(t-t')/\tau)}{\tau} (1 + \tau f'(x)) P(x, t)$$

$$= D \{1 + \tau f'(x)\} P(x, t)(1 - \exp(-t/\tau))$$

So, the effective Fokker Planck equation upto $O(\tau^2, \exp(-t/\tau))$ is given by

$$\frac{\partial P(x, t)}{\partial t} = -\frac{\partial}{\partial x} f(x) P(x, t) + \frac{\partial^2}{\partial x^2} D_S(x) P(x, t) \tag{1.38}$$

where $D_S(x) = D \{1 + \tau f'(x)\}$.

One must notice that such an approximation does not have uniform convergence in entire

domain of x, i.e., the approximation fails to converge for values of x where $1 + \tau f'(x) < 0$(negative diffusion coefficient). One may derive the same equation from another method developed by Bonilla $et.al$[39], which is described in the Appendix C, which extends to derive higher order terms in a more systematic way.

2. Fox's approximation

This approximation[40] is based on functional calculus methods and produces uniform convergence in the the entire domain of x. The explicit derivation is given below. Substituting Eqn(1.26) into the second term of Eqn(1.30), and making variable change $\theta \equiv (t - t')/\tau$, we get,

$$I \equiv D \int_0^{t/\tau} d\theta \exp(-\theta) \left\langle \delta(x_t - x) \exp\left[\int_{t-\tau\theta}^t dt' f(x_{t'})\right] \right\rangle$$

Now taking the $\tau \to 0$ limit, we get,

$$I \simeq D \int_0^\infty d\theta \exp\left[-\theta + \tau\theta f'(x)\right] \langle \delta(x - x_t) \rangle = \frac{D}{1 - \tau f'(x)} P(x, t)$$

Therefore, the effective Fokker-Planck equation is given by

$$\frac{\partial P(x, t)}{\partial t} = -\frac{\partial}{\partial x} f(x) P(x, t) + \frac{\partial^2}{\partial x^2} D_{\text{fox}}(x) P(x, t) \tag{1.39}$$

where $D_{\text{fox}}(x) = \frac{D}{(1 - \tau f'(x))}$. One can easily show that the small τ expansion corresponds to Sancho's approximation. But this is a better approximation for well-behaved(convex) potential, $f(x) = -\phi'(x)$, as it uniformly converges for the entire domain of x[41]. But again for more complicated potentials, there is a constraint in τ, $1 - \tau f'(x) > 0$ until which the approximation is valid(same range of validity as Sancho's approximation) .

3. Masoliver et.al. approximation

This approximation[42] is based on projection approach to Fokker-Planck equations, valid for small $D\tau$. The generalized Master equation upto $O(D\tau)$ for $P_t \equiv P(x, t|x_0)$, where x

17

from projector approach, is given by

$$\frac{\partial P_t}{\partial t} = L_0 P_t + \int_0^t ds \langle L_f(t) \exp(L_o s) L_f(t-s) \exp(-L_0 s) \rangle P_t [1 + O(D\tau)] \tag{1.40}$$

such that the deterministic evolution operator is given by

$$L_0(t) \equiv -\frac{\partial f(x)}{\partial x} \tag{1.41}$$

and the stochastic evolution operator is given by

$$L_f(t) \equiv -\xi(t) \frac{\partial}{\partial x} \tag{1.42}$$

After some algebraic manipulations and using exponential identity for operators, $\exp(A)B\exp(-A) = B + [A, B] + \frac{1}{2!}[A, [A, B]] + \dots$ we obtain,

$$\frac{\partial P(x,t)}{\partial t} = -\frac{\partial}{\partial x} f(x) P(x,t) + \frac{\partial^2}{\partial x^2} D_{\text{Masoliver}}(x,t) P(x,t) \tag{1.43}$$

where $D(x,t) = \int_0^t ds \Gamma(s) \sum_{n=0}^{\infty} \frac{\tau^n}{n!} F_n(x)$ such that each F_n satisfies a recurrence relation given by

$$F_n(x) = f'(x) F_{n-1} - f(x) F'_{n-1}(x) \tag{1.44}$$

with $F_0(x) = 1$. The key point in the approximation is to find a closed form solution of the summation. The above method is also valid for any Gaussian noise statistics. For the case of Gaussian colored noise, assuming that the time scale of observation is much larger than τ, we obtain a closed form for the $D(x,t) \sim D(x)$, given by

$$D_{\text{Masoliver}}(x) = D \left[1 + \frac{\tau f(x)}{1 - \tau f'(x)} \frac{d}{dx} \right]^{-1} \left(\frac{1}{1 - \tau f'(x)} \right) \tag{1.45}$$

From the above form for Diffusion coefficient, we can obtain the above approximation by ignoring the first term, with inverse of the derivative. So, even for small $D\tau$, we see that the space dependent diffusion has higher order derivatives of the potential and the probability density, which deviates from the usual Fokker-Plank equation.

4. Unified Colored Noise Approximation(UCNA)

This approximation[43] converts the non-Markovian dynamics to Markovian dynamics at the trajectory level, using adiabatic approximation to eliminate momentum degrees of freedom. Working in the phase space of $(x, \dot{x})$, one obtain the following Langevin equation with space dependent friction, given by

$$\ddot{x}_t + \underbrace{(\tau^{-1} - f'(x_t))}_{\gamma(x,\tau)} \dot{x}_t = \frac{f(x_t)}{\tau} + \frac{\sqrt{2D}}{\tau}\eta_t \tag{1.46}$$

where the space dependent damping coefficient is given by $(\tau^{-1} - f'(x))$ and $\eta(t)$ is white noise with normal distribution.

Rescaling time, $\tilde{t} = t\tau^{-1/2}$, we obtain,

$$\ddot{x}_t + \gamma_{\text{eff}}(x_t, \tau)\dot{x}_t = f(x_t) + \frac{\sqrt{2D}}{\tau^{1/4}}\eta_t \tag{1.47}$$

where the new damping coefficient is given by

$$\gamma_{\text{eff}}(x, \tau) = \tau^{-1/2} + \tau^{1/2}[-f'(x)] \tag{1.48}$$

Now, one may identify that the $\gamma_{\text{eff}}(x, \tau)$ small limit, when the correlation time, $\tau \to 0$ and $\tau \to \infty$. This implies that one can do an adiabatic approximation to eliminate the inertia term, thus giving,

$$\dot{x}_t = \frac{f(x_t)}{\gamma(x_t, \tau)} + \left[\frac{(2D\tau^{-1/2})^{1/2}}{\gamma(x_t, \tau)}\right]\eta_t \tag{1.49}$$

The corresponding Fokker-Planck equation,in the original time scale, for the above Langevin equation is given by

$$\frac{\partial P(x,t)}{\partial t} = -\frac{\partial}{\partial x}\left[\frac{f(x)P(x,t)}{(1 - \tau f'(x))}\right] + \frac{\partial}{\partial x}\frac{1}{(1 - \tau f'(x))}\frac{\partial}{\partial x}\frac{P(x,t)}{(1 - \tau f'(x))} \tag{1.50}$$

Even though, the above approximation has different Fokker Planck equation compared to the Fox's approximation, the equilibrium distribution $f(x) = -\phi'(x)$ is the same. But, we will see that, its not the case when there is non-zero current in the steady state. Since, this approximation works for both small τ as well as large τ limit, it should be a better approximation for intermediate τ values.

One of the important approximations that go into this system is that adiabatic approximation works only when the damping coefficient is positive and large, i.e.$\gamma(x, \tau) \gg 0$. Therefore, one obtains a similar bound on the correlation time, τ dependent on the system. Similarly, the approximation holds only on time scales when $t > \tau^{1/2}\gamma^{-1}$ and also the time scale should be also that the drift forces are not varying appreciably over the characteristic length scale associated with diffusion, i.e,

$$\gamma(x, \tau) \gg D^{1/2}\left|\frac{f'(x)}{f(x)}\right| \tag{1.51}$$

5. Interpolation Approximation

This approximation[44] can be considered an extension of UCNA, as it tries to form an interpolation between the two limits. $\tau \to 0$ and $\tau \to \infty$. Let us define an interpolation "motility" function, $\theta[\tau f'(x)]$, such that it satisfies the limits acquired in UCNA, i.e.,

$$\lim_{\tau \to 0} \theta[\tau f'(x)] = 1 \tag{1.52}$$

and

$$\lim_{\tau \to 0} \theta[\tau f'(x)] = -[\tau f'(x)]^{-1} \tag{1.53}$$

Therefore the Interpolation Fokker-Planck equation will be given by

$$\frac{\partial P(x,t)}{\partial t} = -\frac{\partial}{\partial x}\left[\frac{f(x)P(x,t)}{(1 - \tau f'(x))}\right] + \frac{\partial}{\partial x}\frac{1}{(1 - \tau f'(x))}\frac{\partial}{\partial x}\frac{P(x,t)}{(1 - \tau f'(x))} \tag{1.54}$$

For the case of UCNA, interpolation function takes the form, $\theta[\tau f'(x)] = [1 - \tau f'(x)]^{-1}$. So,this approximation opens up the possibilty to have better Markovian approximations compared to UCNA, with a system dependent interpolation function. One such family of function, which also includes UCNA is given by

$$\theta[\tau f'(X)] = \frac{1 - c[\tau f'(x)]^{n-1}}{1 + c[\tau f'(x)]^n} \tag{1.55}$$

where c and n are fitting parameters.

It can be also used to determine a better form of stationary distribution in the domain of phase space where the damping is negative(accelerating), compared to UCNA where it fails. This approximation has been successfully used to determine the stationary distribution for

20

Langevin dynamics in symmetric double well potential driven by colored noise[44].

Stochastic thermodynamics in Active Baths

Considering the motion of a Brownian tracer in active bath in the overdamped limit, we will define $f(x) = \frac{1}{\gamma}(F_{nc} - \phi'(x,t))$, where F_{nc} corresponds to a constant non-conservative force[45]. Following the Sekimoto's definition, the work done on the system is given by

$$\delta W_t = \frac{\partial \phi}{\partial t}dt + F_{nc} \circ dx_t \tag{1.56}$$

Similar to the definition of heat in the thermal bath, one can consider active fluctuations to be another source of fluctuations.Hence heat inputted into the system is given by

$$\delta Q_t = (-\gamma \dot{x}_t + \xi_t) \circ dx_t = (F_{nc} - \phi'(x,t)) \circ dx_t \tag{1.57}$$

The internal energy of the system is defined by $U = \phi(x,t)$ and hence one can easily obtain First Law of thermodynamics at the trajectory level, given by

$$dU = \delta Q + \delta W \tag{1.58}$$

Probability $P(\underline{x}|x_0)$ to observe a particular trajectory, $\underline{x} = \{x(t')\}_{0<t'<\mathcal{T}}$ with initial condition at x_0 can be directly obtained by the extension of Onsager-Machlup path integral method to non-Markovian Gaussian noise[46]. For a Gaussian colored noise,

$$P[\tilde{\underline{\xi}}|\xi_0] \propto \exp\left[-\frac{1}{2}\int dt \int ds\xi(s)\Gamma^{-1}(t-s)\xi(t)\right]$$

where Γ^{-1} is the inverse of the auto-correlation function,Γ ,defined as,

$$\int dt'\Gamma^{-1}(t-t')\Gamma(t'-s) = \delta(t-s) \tag{1.59}$$

For the colored noise, one obtains $\Gamma^{-1}(t-s) = \frac{\delta(t-s)}{2D}\left(1 - \tau^2\frac{d^2}{dt^2}\right) \equiv \delta(t-s)G^{-1}(t)$, working in the Fourier space and then inverting it back, which is local in time.

After changing variables one can obtain the path probability,$P[\underline{x}|x_0]$, assuming that noise

is already in the stationary distribution, to be given by

$$P[\underline{x}|x_0] \propto \exp\left[-\frac{1}{2}\int dt \int ds(\dot{x}_s - f(x_s))\Gamma^{-1}(t-s)(\dot{x}_t - f(x_t)) - \frac{f'(x_t)}{2} - \tau\frac{[\dot{x}_0 - f(x_0)]^2}{2D}\right] \quad (1.60)$$

After some manipulation, we obtain,

$$P[\underline{x}|x_0] \propto \exp\left[-\left(\int \frac{[(1+\tau d_t)(\dot{x}_t - f(x_t))]^2}{4D} - \frac{f'(x_t)}{2} - \tau\frac{[\dot{x}_0 - f(x_0)]^2}{2D}\right)\right] \quad (1.61)$$

We can see that Lagrangian-like function, depends on $\ddot{x}$ due to non-Markovian nature of the bath. Now, to compute the amount of irreversiblity, we compute the path probability for the time reversed trajectory,$P[\Theta\underline{x}|\Theta x_0]$, after dropping the last two terms from Eqn(1.59), as they either contribute to boundary terms or can ignored changing convention(Ito or Stratonovich) of defining the path integral, is given by

$$P[\Theta\underline{x}|\Theta x_0] \propto \exp\left[\frac{1}{2}\int ds \int dt(-\dot{x}_s - f(x_s))\Gamma^{-1}(t-s)(-\dot{x}_t - f(x_t))\right] \quad (1.62)$$

Here, we have implied that Γ^{-1} is even under time reversal transformation(TRT) ,$\Theta \circ (t) = \circ(T-t)$, as the correlation matrix is even under TRT by definition.

Therefore, the entropy production of the environment,$S_{\text{bath}}(\mathcal{T})$, is given by

$$S_{\text{bath}}(\mathcal{T}) = \log\frac{P[\underline{x}|x_0]}{P[\Theta\underline{x}|\Theta x_0]} = \int dt \int ds\left[\dot{x}_t\Gamma^{-1}(t-s)f(x_s) + f(x_t)\Gamma^{-1}(t-s)\dot{x}(s)\right] \quad (1.63)$$

where we have dropped the boundary terms,$\dot{x}\Gamma^{-1}\dot{x}$ and $f\Gamma^{-1}f$ and defining $f*g(t) \equiv \int_{-\infty}^{\infty} f(t-s)g(s)ds$, as the convolution operator, we get a simplified form for the time dependent entropy production rate,

$$\sigma(t) = \dot{x}_t\left(\Gamma^{-1}*f(x)\right)(t) + f(x_t)\left(\Gamma^{-1}*\dot{x}\right)(t) \quad (1.64)$$

$$= \frac{1}{D\gamma}\left(F_{nc}\dot{x}_t - \frac{d\phi}{dt}(t)\right) + \frac{\tau^2}{2D\gamma}\left[\dot{x}^3\phi'''(t) + \frac{d}{dt}\left(\ddot{x}_t\phi'(t)\right)\right] \quad (1.65)$$

The entropy production of the active bath cannot be easily mapped to the thermodynamic quantities, due to the presence of memory, as in the case of the thermal bath. The first term corresponds to the heat expelled by the system in the active bath. But, here we see that there is also entropy production due to active nature of the bath.

In the steady state, the entropy production rate can be obtained by averaging over the stationary distribution, i.e. $\mathcal{T} \to \infty$, and assuming ergodicity, we get,

$$S_{\text{bath}}(\mathcal{T}) \sim \mathcal{T}\langle \sigma \rangle = \mathcal{T} \int dx P_s(x) \sigma(\mathcal{T}) \tag{1.66}$$

Interestingly, for "equilibrium"(zero current) systems, it can shown that the contributions of average entropy production occur at the lowest order τ^2, i.e. $\langle \sigma \rangle \sim T\tau^2 \langle (\phi''')^2 \rangle$ for small τ [47]. So the system is effectively "equilibrium"(non-thermal) system for small correlation times.

To compute the dissipation in the active bath, one may extend the definition of Sekimoto, i.e. the imbalance of power injected by drag force and power dissipated through the viscous force, given by

$$
\begin{aligned}
I & = \dot{x}\Gamma^{-1}f(x) = -\dot{x}\Gamma^{-1}\dot{x} + \dot{x}\Gamma^{-1}\xi \\
& = \frac{\dot{x}(F_{nc} - \phi')}{\gamma^2 D} + \frac{\tau^2}{2D\gamma^2}\left[\dot{x}\frac{d^2\phi'}{dt^2} + \phi'\frac{d^2\dot{x}}{dt^2}\right]
\end{aligned}
$$

$$\tag{1.67}$$
$$\tag{1.68}$$

For the ease of notation, I have dropped the time subscript and convolution operator. One may also identify that the above dissipation can be related to entropy production via,

$$\sigma = I + I^{\text{adj}} \tag{1.69}$$

Chapter 2

Adler oscillator in an Active Bath

Let us consider the dynamics of a non-uniform oscillator in the presence of an active bath, i.e. a large reservoir of active particles. The dynamics of the system can be captured by a Langevin equation given below,

$$I\ddot{\theta}_t + \gamma\dot{\theta}_t \;\;=\;\; f - k\sin\left(\frac{2\pi\theta_t}{L}\right) + \xi_t \tag{2.1}$$

$$\langle\xi_t\rangle = 0, \langle\xi_t\xi_{t'}\rangle \;\;=\;\; \Gamma(t - t') = \frac{2\gamma k_B T_{\text{eff}}}{\tau}\exp\left(-|t - t'|/\tau\right) \tag{2.2}$$

where θ_t is the phase of the oscillator with periodic boundary conditions, $\theta_t + L = \theta_t$ such that L is the periodicity of oscillator , I is the moment of inertia, γ is the friction coefficient , f is the external driving torque(non-conservative), k is the strength of the non-linear potential and $\Gamma(t - t')$ is the auto-correlation function of the noise.

The choice of this non-linear potential is motivated by many physical and biological systems. For example, in the case of Josephson junctions, Kirchoff's law of current and voltage balance gives the above equation in the presence of a capacitor and resistor. Similarly, one finds the same equation for a pendulum under the effect of an external torque f in the presence of gravitational force. One of the other key application corresponds to the phenomenon of synchronization, which has many application in physical systems like power grids[48], where AC frequency of generator has to be matched with the entire grid for least power loss and biological systems like synchronization between cilia for cellular propulsion[49]. One of the pragmatic models used to study this phenomenon is Kuramoto

model and Eqn. (2.1) corresponds to the mean field limit of the Kuramoto model in the presence of inertia and noise. There are many other applications in biological systems like intra-cellular transport (simplest model for Brownian motors), phase locking in hair bundles in the hair cells to an external signal etc.[]

Some of the key assumptions that go into this model is that we would like to study the system away from detailed balance, due to the presence of active bath. The above model doesn't satisfy fluctuation-dissipation theorem of second kind[50], $\Gamma(t - t') = k_B T \gamma(|t - t'|)$, which guarantees canonical distribution in bath with temperature T, as here we assume that the viscosity kernel is a delta function, i.e., $-\int_{-\infty}^{t} \gamma(t - t') \dot{\theta}_{t'} dt' \rightarrow -\gamma \dot{\theta}_t$.

We also assume that the effect of a thermal bath is negligible compared to the activity of the active bath, which has been experimentally confirmed for some bacterial colonies in pure water[35, 36]. The active collisions withe bacteria plays a stronger role in the dynamics compared to the thermal collisions with the solvent.

We will consider the noise statistics due to the presence of active bath to be of Gaussian distribution with the following form,

$$\Gamma(t - t') = \frac{C}{2\tau} \exp(-|t - t'|/\tau) \tag{2.3}$$

where τ is the correlation/persistence time of the active particles on the passive tracer and $C = 2\gamma k_B T_a$ is the strength of strength of active noise. We have defined the strength in this particular form to make easier connection with the case of thermal bath, where fluctuation-dissipation relation holds. We can also identify that the noise statistics corresponds to the active dynamics typically studied using Run & Tumble dynamics, Active Ornstein-Uhlenbeck dynamics etc.

2.1   Nonlinear deterministic driven oscillator

Let us first consider the case where we neglect the fluctuation produced by the bath, i.e. when $C = 0$. In this case, the dynamics is well studied and known as the Adler dynamics, a model used to study non-uniform oscillations.

26

2.1.1 Overdamped Case:

Let us first case consider the simpler case of one dimensional flow with periodic boundary conditions, i.e. neglecting the effect of inertia (Overdamped limit). This limit is usually taken when the moment of inertia is very low or in a highly viscous, i.e. $I/\gamma \gg 1$ The corresponding equation of motion in adimensional form is given by

$$\dot{\theta} = a - \sin(\theta) \tag{2.4}$$

such that $a = \frac{f}{k}$ and dimensionless time, $t \to \frac{2\pi f}{L\gamma}t$ and phase, $\theta \to \frac{2\pi}{L}\theta$.

Linear stability analysis on this system gives that for $a < 1$ the system has both a stable fixed point, $\theta^* = \arccos(\sqrt{1-a^2})$ and an unstable fixed point, $\theta^* = \arccos(-\sqrt{1-a^2})$ for $0 \leq a \leq 1$, where the both stable and unstable fixed points converge to become a saddle point at $\theta^* = \pi/2$. The dynamics asymptotically goes to a stable fixed point when $0 < a = \frac{f}{k} < 1$, whereas when $a > 1$ the system just keeps on oscillating with non-uniform frequency based on the phase of the oscillator, which we call the "running state". The system undergoes saddle-node bifurcation at $\theta^* = \pi/2$, which is also the dynamical bottleneck.
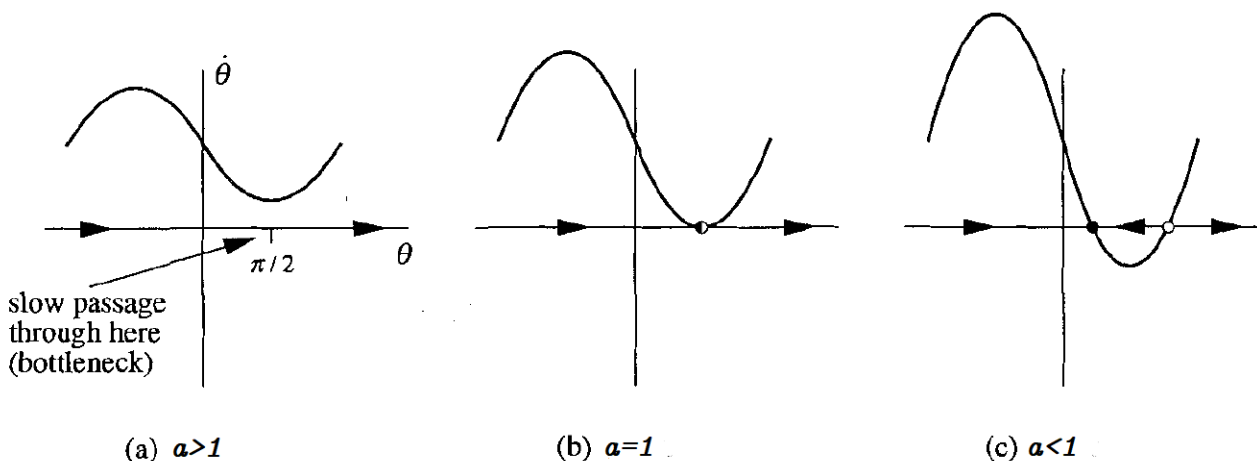

Figure 2.1: 1 dimensional flow for the overdamped Adler dynamics representing Saddle node bifurcation at $\theta^* = \pi/2$

Above the bifurcation point (i.e. $f > k$), the system oscillates non-uniformly in the phase space. The time period of the oscillator, time required to complete one oscillation,

can be computed as follows,

$$T_{adler} = \int dt = \int_0^{2\pi} \frac{dt}{d\theta} d\theta = \int_0^{2\pi} \frac{1}{a - \sin\theta} d\theta \tag{2.5}$$

$$= \frac{2\pi}{\sqrt{a^2 - 1}} \tag{2.6}$$

This implies in the usual dimension, the average frequency(averaged over a cycle) of the system is given by

$$\langle \dot\theta_a \rangle = \begin{cases} 0 & , f \leq k, \\ \sqrt{\left(\frac{f}{k}\right)^2 - 1} & , f > k \end{cases} \tag{2.7}$$

$$\tag{2.8}$$

One can easily identify that as $f \to k^+$, the time period of the system diverges, which is the reason for the dynamical bottleneck, and there exist the average frequency is non-analytic at $f = k$.

2.1.2 Underdamped Case:

Now let us consider the original dynamical problem, with inertia(underdamped limit). The corresponding equation of motion after non-dimensionalizing is given by

$$\ddot\theta_t + G\dot\theta_t = a - \sin\theta_t \tag{2.9}$$

where $G = \frac{\gamma}{\sqrt{kI}}$, $a = \frac{f}{k}$ and to non-dimensionalize, we use $t \to \sqrt{\frac{k}{I}\frac{2\pi}{L}}$, $\theta \to \theta\frac{2\pi}{L}$.

We can therefore write the equation of motion as dynamics in 2 dimensional phase space of $(\theta, z = \dot\theta)$, which corresponds to motion in a cylinder (due to periodic boundary conditions on θ), given by

$$\dot\theta_t = z_t \tag{2.10}$$

$$\dot z_t = a - \sin\theta_t - Gz_t \tag{2.11}$$

Using linear stability analysis, one can find that for $a < 1$, there exist both stable and unstable fixed points. The stable fixed point is a stable node if $G^2 - \frac{8\pi}{L}\sqrt{1 - a^2} > 0$, else

the fixed point is a stable spiral. Again, we have saddle-node bifurcation of fixed points at $a = \frac{f}{k} = 1$, i.e. the stable and unstable fixed point coalesce to saddle point at the bifurcation point.

When $a > 1$, it can be easily shown that the system asymptotically converges to unique stable limit cycle. So, for large values of G, i.e. high damping limit, there exists an infinite period bifurcation, similar to the one in over-damped limit, where the near the bifurcation point the time period of the limit cycle diverges, resulting in the formation of stable and unstable node. Moreover, this system also has a bistable region for small damping and $a < 1$, i.e. the system has asymptotically two stable regions in the phase space associated with a stable node and stable limit cycle (Interestingly, with different topological features). The last bifurcation that the system has is the homoclinic bifurcation, where the limit cycle expands as one gets closer to the bifurcation point, when it finally gets destroyed when it crosses saddle point, through a homoclinic orbit. The differences between all these bifurcations are on the different scaling relations on the time period and amplitudes of the oscillations as discussed in Sec. 1. The resulting bifurcation diagram of the system is shown below,
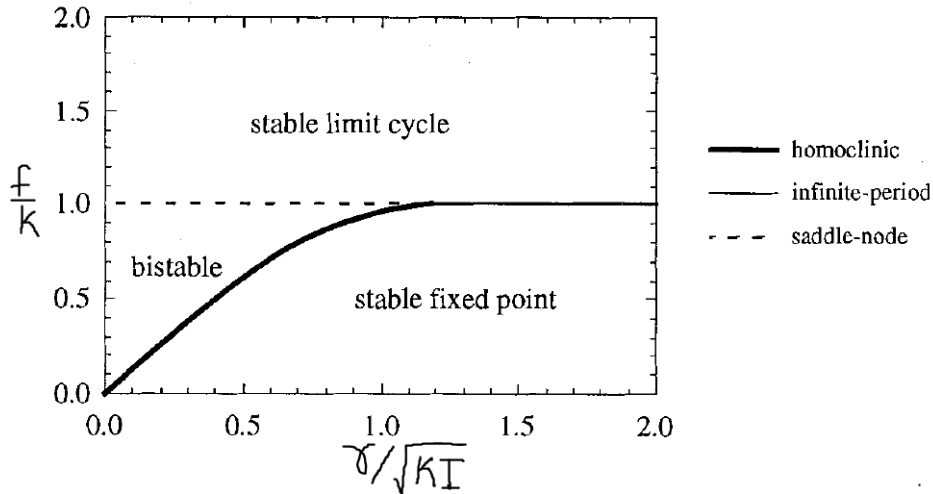

Figure 2.2: Bifurcation Diagram for the underdamped Adler Dynamics.Taken from [27]

One of the interesting consequence of presence of bistability is the presence of hysteresis effects when goes through bistability region from the different basin of attraction, at fixed $G = \gamma/\sqrt{kI}$ and f. Here, for example, for small damping cases, when one initially start from the external torque from small values, the system is asymptotically found at the stable node. When one changes adiabatically increase a, the system continues to be at the stable node until it reaches the saddle node bifurcation point of fixed points at $a = 1$, after which the

system suddenly jumps into the limit cycle solution and stays there with further increase of a. Now, when one adiabatically decrease a, the system continues to stay in limit cycle solution with decreasing frequency, even in the bistable region, until the homoclinic bifurcation point, when it jumps back to stable node solution.

2.2 Nonlinear stochastic driven oscillator in a thermal bath

In the limit of very small correlation time, i.e. $\tau \ll \Delta t$(observation time scale), the system behaves as memory-less and one can identify that thermal(passive) bath is the zero correlation time limit of the of the active bath, i.e.,

$$\lim_{\tau \to 0} \Gamma(|t - t'|) = \lim_{\tau \to 0} \frac{2\gamma k_B T_{\text{eff}}}{2\tau} \exp(-|t - t'|/\tau) = 2\gamma k_B T \delta(|t - t'|) \tag{2.12}$$

where the effective temperature is the temperature of the bath itself.

Let us consider the above oscillator in the presence of the isothermal bath, i.e. a large reservoir of solvent(passive) particles with temperature T.The corresponding Langevin equations is given by

$$I\ddot{\theta}_t + \gamma\dot{\theta}_t = \qquad f - k\sin\left(\frac{2\pi\theta_t}{L}\right) + \eta_t \tag{2.13}$$

$$\langle\eta_t\rangle = 0, \langle\eta_t\eta_{t'}\rangle = \Gamma(t - t') = 2\gamma k_B T\delta(|t - t'|) \tag{2.14}$$
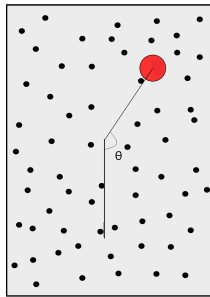

Figure 2.3: Adler Dynamics in a Thermal Bath

The coarse grained effect of large number of collisions with the bath particles can be captured by Gaussian white noise. The above system satisfies fluctuation-dissipation relation, and hence Einstein relation, which relates the strength of the fluctuations to the coefficient of viscosity. Hence, we can define diffusion coefficient which corresponds to the variance in displacement in the absence of the potential, to be given by

$$D = \frac{k_B T}{\gamma}. \tag{2.15}$$

To compute the statistics of thermodynamic quantities, we use the formalism of stochastic thermodynamics discussed in Sec. 1. Let us formally write the stochastic differential equation(SDE) of the above model(underdamped) in the Stratonovich sense, given by

$$d\theta = \frac{p}{I} dt \quad , dp = \left(f - k \sin \frac{2\pi\theta}{L}\right) dt - \gamma \frac{p}{I} dt + \sqrt{2\gamma k_B T} \circ dB_t \tag{2.16}$$

Even though the phase of the oscillator has periodic boundary conditions, for a proper description of the thermodynamic quantities defined at the trajectory level, one has to work with the real line extension of the phase variable, i.e. $\theta \in [0, 2\pi] \to x \in (-\infty, \infty)$. We have to work in such variables, to make sure that heat and work are continuously defined when the particle crosses the boundary. In the real line variables, the thermodynamic quantities are given by

$$d'W_t \equiv f \circ dx_t \tag{2.17}$$

$$d'Q_T \equiv \left(-\gamma \frac{p}{I} + \eta(t)\right) \circ dx_t \tag{2.18}$$

$$U_t \equiv \frac{p_t^2}{2I} - \frac{kL}{2\pi} \cos\left(\frac{2\pi x_t}{L}\right) \tag{2.19}$$

which statisfy the first law at the trajectory level, i.e. $dU_t = d'W_t + d'Q_t$

2.2.1 Overdamped limt

In the limit when the momentum relaxation time, I/γ is very small compared to the observational time scales, one can assume that the momentum to be relaxed to its stationary distribution, and hence neglect the term, $I\ddot{\theta}$. The corresponding one-dimensional stochastic

differential equation(SDE) is given by,

$$\gamma d\theta_t = \left(f - k\sin\left(\frac{2\pi\theta}{L}\right) \right) dt + \sqrt{2\gamma k_B T} \circ dB_t \qquad (2.20)$$

Since the above stochastic differential equation is non-linear, it is usually easier to work at the level of ensemble to compute the statistics of different thermodynamic quantities, because Fokker-Planck equation is linear partial differential equation with non-linear coefficients. The Fokker-Planck equation for the overdamped dynamics is given by

$$\frac{\partial P}{\partial t}(\theta, t) = -\frac{1}{\gamma}\frac{\partial}{\partial \theta}\left[\left(f - k\sin\left(\frac{2\pi\theta}{L}\right) \right) P(\theta, t) \right] + D\frac{\partial^2 P}{\partial \theta^2}(\theta, t) \quad . \qquad (2.21)$$

with boundary conditions $P(\theta, t) = P(\theta + L, t)$ and the normalization condition $\int_0^L P(\theta, t)d\theta = 1$.

We are interested in computing the steady state properties of the above system. So from now on, all the statistics of different quantities are computed with respect to steady state distribution, given by $\frac{\partial P}{\partial t} = 0$ and the probability current,$J(\theta)$ is given by

$$J(\theta) = \left(a - b\sin\left(\frac{2\pi\theta}{L}\right) \right) P(\theta) - \frac{\partial P}{\partial \theta} = C_1 \qquad (2.22)$$

J is constant and independent of phase in the steady state. We have also introduced new notation for ease of calculations,

$$a \equiv \frac{f}{\gamma D}, \quad b \equiv \frac{kL}{2\pi\gamma D} \qquad (2.23)$$

Since, the system is periodic in θ, we can impose periodic boundary condition along with the normalization condition,

$$P(\theta, t) = P(\theta + L, t), \quad \int_0^L P(\theta)d\theta = 1 \qquad (2.24)$$

A general solution for Eqn (2.21) with the above boundary conditions in the stationary state, is given by

$$P_s(\theta) = C_1 \exp\left[a\theta + b\cos\left(\frac{2\pi\theta}{L}\right) \right] \int_{C_2}^{\theta} \exp\left[-\left(a\phi + b\cos\left(\frac{2\pi\phi}{L}\right) \right) \right] d\phi \qquad (2.25)$$

where C_1 and C_2 are the arbitrary constants.For satisfying the boundary conditions, we have to take $C_2 = \infty$ or $C_2 = -\infty$. Here we will take former case,

$$P_s(\theta + L) = C_1 \exp\left[La\right] \exp\left[a\theta + b\cos\left(\frac{2\pi\theta}{L}\right)\right] \int_\infty^{\theta+L} \exp\left[-\left(a\phi + b\cos\left(\frac{2\pi\phi}{L}\right)\right)\right] d\phi$$

$$= C_1 \exp\left[La\right] \exp\left[a\theta + b\cos\left(\frac{2\pi\theta}{L}\right)\right] \int_\infty^{\theta} \exp\left[-\left(a(\phi' + L) + b\cos\left(\frac{2\pi\phi'}{L}\right)\right)\right] d\phi'$$

$$= P_s(\theta)$$

Now rearranging the above formula ,

$$P_s(\theta) = C_1 \exp\left[La\right] \exp\left[a\theta + b\cos\left(\frac{2\pi\theta}{L}\right)\right] \int_\infty^{\theta+L} \exp\left[-\left(a\phi + b\cos\left(\frac{2\pi\phi}{L}\right)\right)\right] d\phi \quad (2.26)$$

$$= C_1 \exp\left[La\right] \exp\left[a\theta + b\cos\left(\frac{2\pi\theta}{L}\right)\right] \left[\int_\theta^{\theta+L} \exp\left[-\left(a\phi + b\cos\left(\frac{2\pi\phi}{L}\right)\right)\right] d\phi\right.$$

$$\tag{2.27}$$

$$\left. + \int_{\theta-L}^{\theta} \exp\left[-\left(a\phi + b\cos\left(\frac{2\pi\phi}{L}\right)\right)\right] + ...\right] d\phi \tag{2.28}$$

$$= \frac{1}{N} \exp\left[a\theta + b\cos\left(\frac{2\pi\theta}{L}\right)\right] \int_\theta^{\theta+L} \exp\left[-\left(a\phi + b\cos\left(\frac{2\pi\phi}{L}\right)\right)\right] d\phi \tag{2.29}$$

$$\tag{2.30}$$

where N is given by

$$N = -\frac{(1 - \exp\left[-La\right])}{C_1} \tag{2.31}$$

Let us fix C_1 by using the normalization condition,

$$N = \int_0^L d\theta \int_\theta^{\theta+L} d\phi \exp\left[a\theta + b\cos\left(\frac{2\pi\theta}{L}\right)\right] \exp\left[-\left(a\phi + b\cos\left(\frac{2\pi\theta}{L}\right)\right)\right] \tag{2.32}$$

Making a variable change $\psi = \phi - \theta$, we get,

$$N = \int_0^L d\theta \int_0^L d\psi \exp\left[a\theta + b\cos\left(\frac{2\pi\theta}{L}\right)\right] \exp\left[-(a(\psi+\theta) + b\cos\left(\frac{2\pi(\theta+\phi)}{L}\right))\right]$$

$$= \int_0^L d\theta \int_0^L d\psi \exp\left[-a\psi + 2b\sin\left(\frac{2\pi}{L}\psi/2\right)\sin\left(\frac{2\pi}{L}(\theta+\psi/2)\right)\right]$$

$$= \frac{L^2}{2\pi}\int_0^{2\pi} d\psi' \exp[-a'\psi']I_0[2b\sin(\psi'/2)]$$

The last integral only converges when $L = 2n\pi$ where $n \in \{1,2,3...\}$ .Now making another variable change $y = 1/2*(\pi - \psi')$ for $0 < \psi' < \pi$ and $y = 1/2(\psi - \pi)$ for $\pi < \psi' < 2\pi$, and $a' = \frac{2\pi}{L}a = \frac{Lf}{2\pi\gamma D}$

$$N = \frac{2L^2}{\pi}\exp\left[-La/2\right]\int_0^{\pi/2} dy \cosh(2a'y)I_0(2b\cos(y)) \tag{2.33}$$

We will use a result from Handbook of Ryzhik and Gradstein[51] (Eqn. 6.681.3), which gives us,

$$N = L^2 \exp\left[-La/2\right] I_{ia'}(b)I_{-ia'}(b) \tag{2.34}$$

where the $I_{ia}(b)$ is a^{th} order modified Bessel function of first kind with imaginary order and real argument, b.

We derived the exact form for the steady state probability current, given by

$$G = \frac{D}{N}(1 - \exp\left[-La\right]) = \frac{2D}{L^2}\sinh\left(\frac{Lf}{2\gamma D}\right)\left|I_{\frac{iLf}{2\pi\gamma D}}\left(\frac{kL}{2\pi\gamma D}\right)\right|^{-2} \tag{2.35}$$

Now using the above results, we can also derive the exact form of average angular frequency in steady state for $L = 2n\pi$,

$$\langle \dot{\theta} \rangle = \left\langle \frac{f}{\gamma} - \frac{k}{\gamma}\sin\left(\frac{2\pi\theta}{L}\right) \right\rangle \tag{2.36}$$

$$= \int_0^{2\pi} d\theta \left[\frac{f}{\gamma} - \frac{k}{\gamma}\sin\left(\frac{2\pi\theta}{L}\right)\right] P(\theta) \tag{2.37}$$

$$= \int_0^{2\pi} d\theta \left[G(\theta) + D\frac{\partial P}{\partial\theta}\right] = LG \tag{2.38}$$

$$= \frac{2D}{L}\sinh\left(\frac{Lf}{2\gamma D}\right)\left|I_{\frac{iLf}{2\pi\gamma D}}\left(\frac{kL}{2\pi\gamma D}\right)\right|^{-2} \tag{2.39}$$

34

From the previous definitions, we can derive an exact form for the average power inputted into the system for $L = 2n\pi$, given by

$$\langle \dot{W} \rangle = f\langle \dot{\theta} \rangle = \frac{2Df}{L} \sinh\left(\frac{Lf}{2\gamma D}\right) \left| I_{\frac{iLf}{2\pi\gamma D}}\left(\frac{kL}{2\pi\gamma D}\right) \right|^{-2} \tag{2.40}$$

where $I_{in}(b)$ is n^{th} order modified Bessel function of first kind with imaginary order and real argument, b. This is the first main result of our work and below we have compared it with the numerical simulations done for the SDE given in Eqn(2.40), and it shows an excellent overlap with the analytical result. As shown in Fig 2.4, with increase in temperature, the average power is always more than the deterministic case, even though the noise is symmetric. This is due to the presence of the external torque which creates an asymmetry in the dynamics, i.e. the fluctuations in the direction of the torque causes the particles to cross the barrier much easier compared to when the fluctuation is in the opposite direction. So, the power inputted into the system could be improved by either increasing the "effective torque", $\frac{(f-k)}{k}$ or decreasing the periodicity of the potential, L or increasing the strength of the noise, D.

In the limit of $D \to 0$, the system approaches the deterministic limit thus we obtain the non-analyticity at the bifurcation point for the average power. Using the properties of Bessel function, one may obtain that the average power in $D \to 0$ limit,

$$\langle \dot{W} \rangle = \begin{cases} 0 & , f \leq k, \\ f\sqrt{\left(\frac{f}{k}\right)^2 - 1} & , f > k \end{cases} \tag{2.41}$$

For the limit, $f \to k$ and $D \to 0$ (Specifically when , $\frac{k}{f} - 1 \sim \frac{1}{2}\left(\frac{\gamma D}{f}\right)^{-2/3}$), we can simplify the Eqn.(2.40)[52],

$$y = \frac{3}{Lx} \left[I_{-1/3}^2(x^{3/2}) + I_{-1/3}^2(x^{3/2}) + I_{-1/3}(x^{3/2})I_{1/3}(x^{3/2}) + I_{1/3}^2(x^{3/2}) \right]^{-1} \tag{2.42}$$

where $x = \left(\frac{fL}{6\pi\gamma D}\right)^{\frac{2}{3}} \left(\frac{k-f}{f}\right)$ and $y = \left(\frac{fL}{6\pi\gamma D}\right)^{\frac{1}{3}} \frac{\langle \dot{W} \rangle \gamma L}{f^2}$.
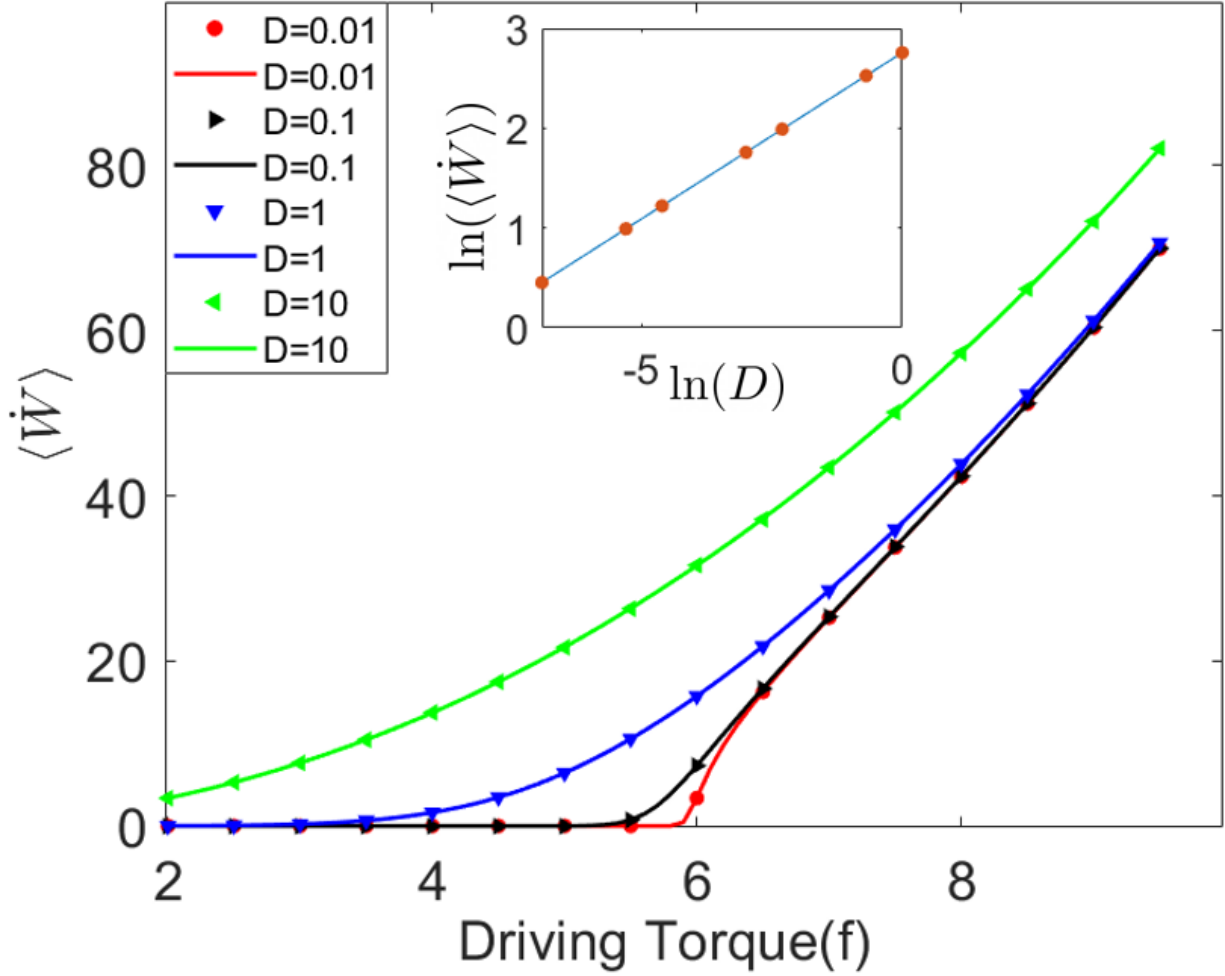
Figure 2.4: The steady state average power inputted into the system with the driving torque for different temperatures($\gamma = 1$). Here the curves correspond to Eqn.(2.40) and the symbols correspond to numerical simulations. We find that the system has finite power below bifurcation point which was 0 for the noiseless case. The inset shows the power law scaling of the average power with the temperature at the critical point

Now, taking $x = 0$, i.e. $f = k$, we get,

$$y = \frac{3}{L} 2^{-\frac{2}{3}} \left[\Gamma \left(\frac{2}{3} \right) \right]^2 \tag{2.43}$$

$$\langle \dot{W} \rangle = \frac{3}{L} 2^{-\frac{2}{3}} \left[\Gamma \left(\frac{2}{3} \right) \right]^2 \left(\frac{f^5}{\gamma^2} \right)^{\frac{1}{3}} (3D)^{\frac{1}{3}} \tag{2.44}$$

where $\Gamma(x)$ is the gamma function. From this, we find that the average power has a scaling form, i.e. $\langle \dot{W} \rangle \propto D^{\frac{1}{3}}$, at the bifurcation and also explains its non-analytic behaviour when

36

$D \to 0$. We have also compared the above result with the numerical calculations in Fig(2.4). We believe that such a scaling form with D depends on the kind of bifurcation and also on the form of the potential near the dynamical bottleneck explained in Section 1.1.

Similarly, one can easily show that in the limit of strong noise, i.e. $D \to \infty$, the equation goes to the limit,

$$\langle \dot{W} \rangle = \frac{f^2}{\gamma} \tag{2.45}$$

This means that in the presence of strong noise, the system can explore freely all the regions of potential that effectively it doesn't feel its presence and the effect of noise will be observed only in its higher moments. It is also interesting that the average power is bounded from both below and above when one increases the temperature of the bath from $T = 0$ to $T \to \infty$.

For the above system, Reimann $et.al.$[53], showed that the effective diffusion coefficient,i.e.,

$$\tilde{D} = \lim_{t \to \infty} \frac{\langle x_t^2 \rangle - \langle x_t \rangle^2}{2t} \tag{2.46}$$

where x is the real line extension of the phase. can be related to the moments of first passage time and the final result, is given by

$$\tilde{D} = D \frac{\int_0^L \frac{dx}{L} I_+^2(x) I_-(x)}{[\int_0^L \frac{dx}{L} I_+(x)]^3} \tag{2.47}$$

where,

$$I_\pm(x) = \int_0^L \frac{dy}{D} \exp\left[(\mp k \cos\theta \pm k \cos(\theta \mp \theta') - \theta f)/D\gamma\right] \tag{2.48}$$

We compared the above result for our model given by Eqn.(2.20)and we got an excellent match with the numerical simulations shown below,
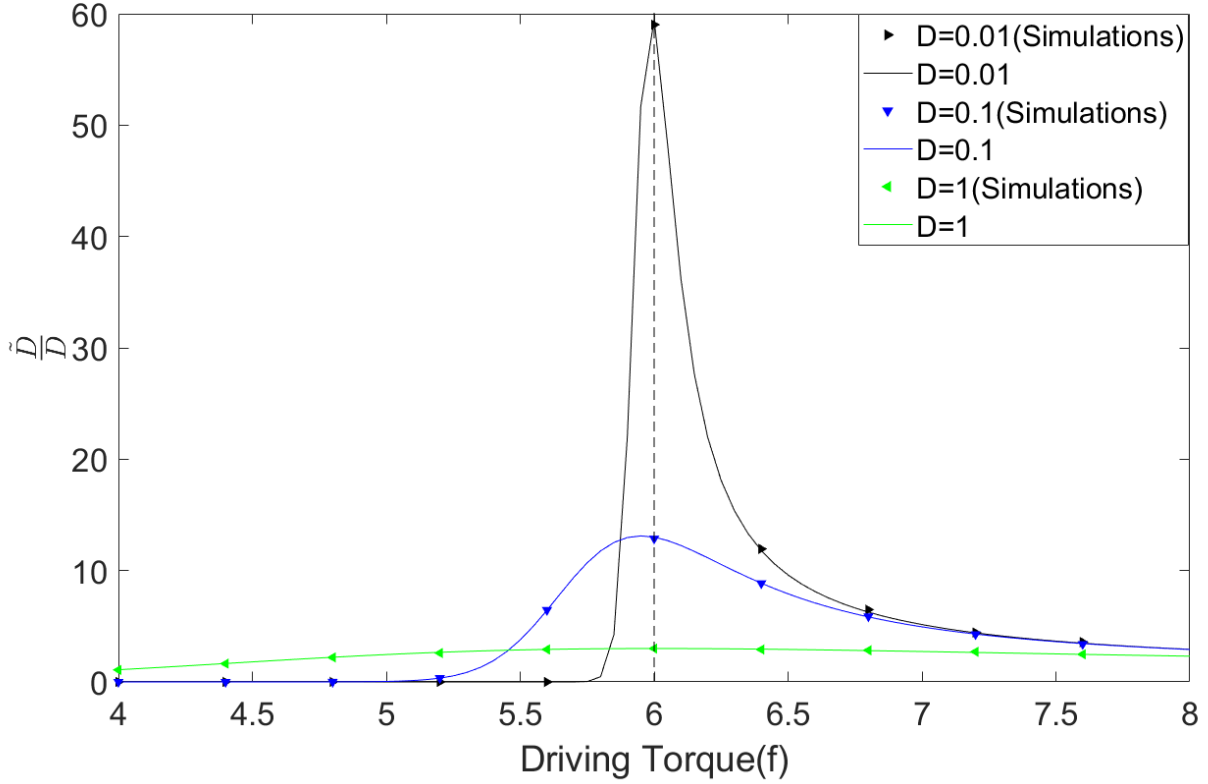
Figure 2.5: Fig 1.Scaled Effective diffusion coefficient,$\tilde{D}/D$ versus the external torque(f) for the Adler system with $L = 2\pi, k = 6, \gamma = 1$ for different temperatures

We can see that there is enhanced effective diffusion at the bifurcation point and enhancement is much more for smaller temperatures. The above effect is due to high instability in the dynamics near the saddle point in the deterministic case and there is high variation compared to the deterministic case for small temperatures w.r.t. higher temperatures. This phenomenon has been called "the giant acceleration" of free diffusion[18].

Now, we would also like to compute the variance in the work inputted into the system in the steady state. Using the definition according to Eqn.(2.17), the variance is given by

$$\text{Var}[W_t] = f^2(\langle x_t^2 \rangle - \langle x_t \rangle^2) \tag{2.49}$$

Using the result Eqn. (2.47), for the variance in the displacement, we can easily derive that

for large times, $t \gg 0$, we get

$$\text{Var}[W_{t \gg 0}] \sim 2f^2 D t \frac{\int_0^L \frac{d\theta}{L} I_+^2(\theta) I_-(\theta)}{\left[\int_0^L \frac{d\theta}{L} I_+(\theta)\right]^3} \tag{2.50}$$
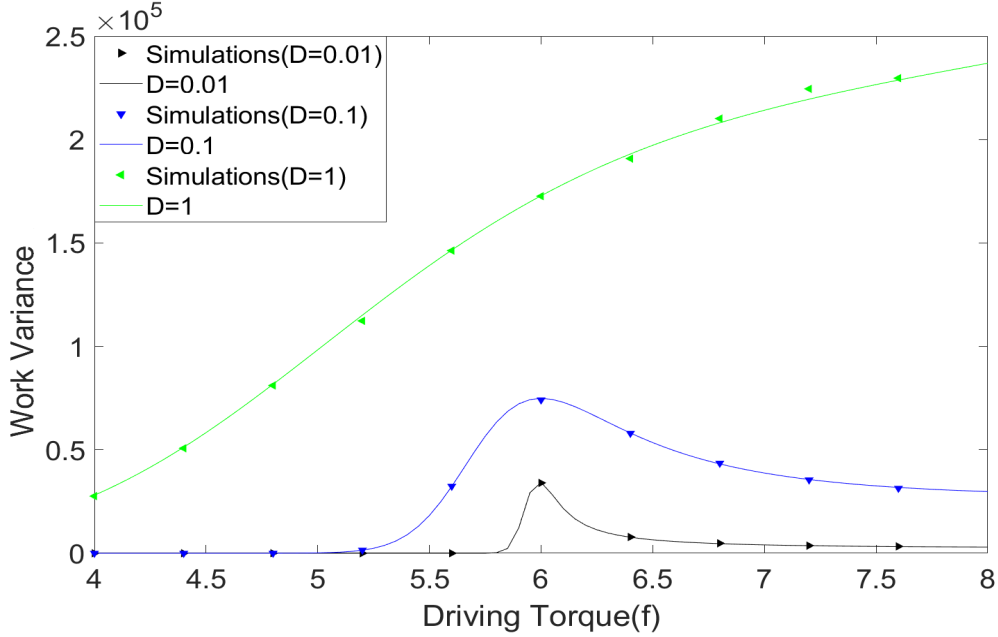

Figure 2.6: Variance in the work inputted into the system at t=800 in the steady state versus the external torque(f) for the Adler system with $L = 2\pi, k = 6, \gamma = 1$ for different temperatures. The curves corresponds to the numerical integration of Eqn.(2.50) for different temperatures

We can see that the above result has good convergence with the numerical simulations(Fig. 2.6). We must identify that the variance in the work inputted into the system, has a peak near the bifurcation point for small temperatures. We also see that with increasing temperatures, the variance also increases as expected. Reimann $et.al.$[53] also derived a scaling form for the Diffusion coefficient for small temperatures. One can easily deduce that $\text{Var}[W_t]$ also has a similar scaling behaviour as average power, i.e. $\text{Var}[W_t] \sim D^{1/3}$, for small values of D. Since, here we are working with fixed friction coefficient γ, small D corresponds to small temperatures T. So energetically, for small temperatures, it is better to go above the

bifurcation point to have maximum output.

To quantify the above we can use the measure called Fano-Factor for the work done till time t, defined as the ration of variance to the mean, given by

$$F_{W_t} = \frac{\text{Var}[W_t]}{\langle W_t \rangle} = 2D \frac{\int_0^L \frac{d\theta}{L} I_+^2(\theta) I_-(\theta)}{\left[\int_0^L \frac{d\theta}{L} I_+(\theta)\right](1 - \exp[-Lf/D\gamma])} \tag{2.51}$$

We have used the fact that the average work done in the system at time t, $\langle W_t \rangle = \langle \dot{W} \rangle t$, since the function is additive in time. We see that the system has highest degree of variation for values below the bifurcation point, which goes towards bifurcation point as $D \to 0$. Hence, for precise input of work into the system, it is better to go far above the bifurcation point.
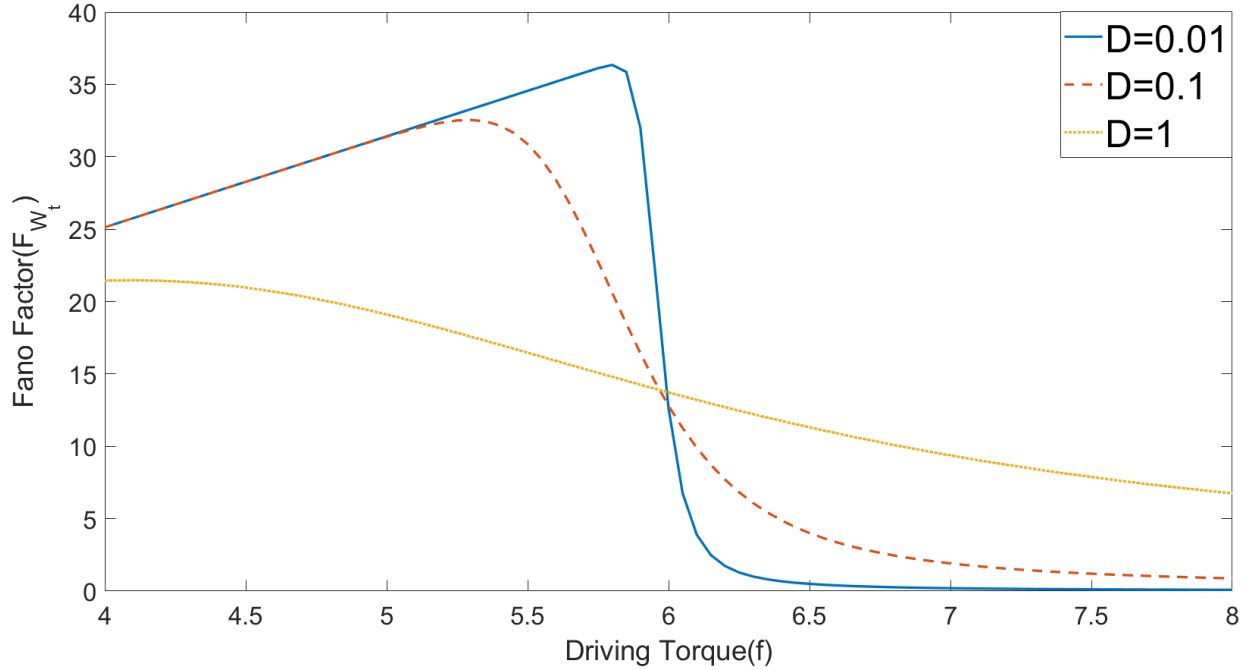

Figure 2.7: Fano factor for the work inputted into the system at t=800 in the steady state versus the external torque(f) for the Adler system with $L = 2\pi, k = 6, \gamma = 1$ for different temperatures. The curves corresponds to the numerical integration of Eqn. (2.51) for different temperatures.

2.2.2 Underdamped limit

The effect of inertia adds a new layer of complexity to the Adler system as discussed in Sec 1.1. The deterministic system is effectively a second order dynamical system with 3 different bifurcations. The addition of thermal fluctuations adds another layer of complexity and below I will discuss the effect on the energetics due to the fluctuations near the bifurcations. The Langevin equation for the Adler dynamics in underdamped case is given by ,

$$I\ddot{\theta}_t + \gamma\dot{\theta}_t = \quad f - k\sin\left(\frac{2\pi\theta_t}{L}\right) + \eta(t) \tag{2.52}$$

where $\langle\eta_t\eta_{t'}\rangle = 2\gamma^2 D\delta(t - t')$.(Using Einstein relation, $D = k_B T/\gamma$)

In this section, we will mainly focus on the Bi-stable region, where the phase space has two stable regions, one for stable node and other for stable limit cycle. The key feature of these two distinct stable solutions are that they are topologically distinct solutions. The stable node solution is characterised by zero angular velocity whereas the stable limit cycle solution is characterized by a finite angular velocity (can still be dependent on the phase). I have below plotted the real line extension of the displacement(x) and angular velocity (v) for a sample trajectory for the parameters in the bi-stable region,

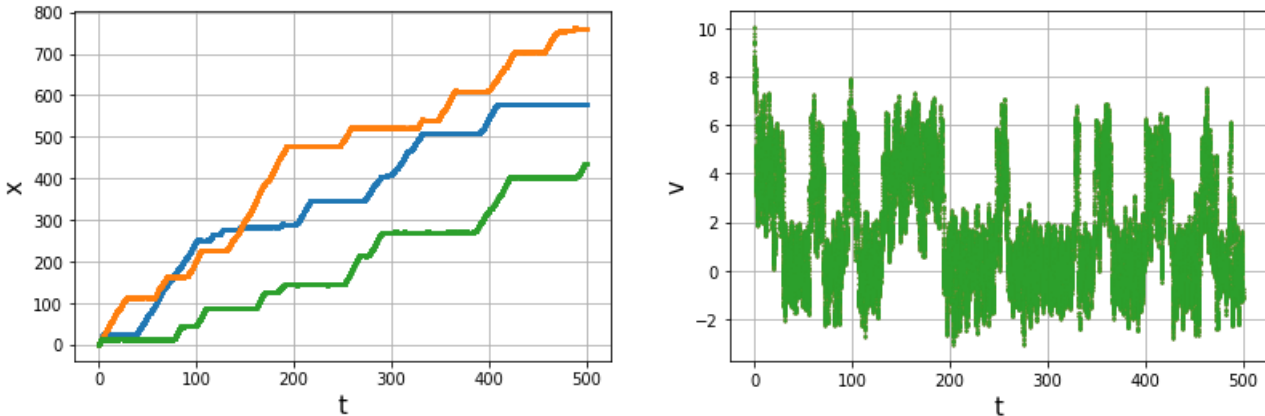
Table 2.1: Left: Real line extension of $\theta(t)$, i.e. $x(t)$ for $f = 4.5, k = 6, D = 0.1$(Bistable region). Right: Angular velocity for same parameter for one of the trajectory(Green)

As you can see the thermal fluctuations help the system to get out of the stability basin of both stable node and stable limit cycle, and hence the trajectories are a mix of the both these trajectories. The key difference between the running state in the overdamped case and

41

the limit cycle in the underdamped case, is in the stability of the solution from the dynamical perspective. In the case of the overdamped case, the running state can suddenly shift to the stable fixed point due to thermal fluctuations around the saddle-node bifurcation point. Whereas in the underdamped case,the presence of bistability implies that one might need bigger thermal fluctuations to move the system out of stability basin.

Stochastic thermodynamics is a tool to analyze the thermodynamic signatures of switching in the trajectory level between the 2 stable solutions, in the thermodynamic quantities. We looked at the average power inputted into the system at large times, to check the effect of bistability, where the we could clearly see the signatures of the two solutions. Below I have plotted the "Hysteresis" plot of the average power with the driving torque. The "Hysteresis" protocol used was as follows: Let the system evolve according to the Langevin equation(Eqn. 2.52) for simulation time,T_{sim} for a value of external torque where the fixed point is the only stable solution, then compute the ensemble average of power inputted into the system. We then proceed to increase the external torque in the direction of bistable region and using the final points as the initial conditions, we again compute the average after T_{sim}.We proceed to use this protocol to increase the external torque(to beyond the saddle-node bifurcation) and then decrease it to cover the entire bistable region. This protocol is the usual 'adiabatic way' to capture Hysteresis behaviour.

As one can notice the hysteresis behaviour still exists in the presence of weak thermal noise, even after large simulation times. This means the system hasn't relaxed to the unique steady state for such large simulation times(limited by the run time). The two averages corresponds to the averages in the stability basin of the two stable solutions. As one can see, the area under the hysteresis curve decreases with increasing temperature.

We can rationalize the hysteresis curve with the Kramer's escape rate from the stability region of both the solutions.We computed the escape time to go from the stability basin of the stable node to the limit cycle solution, using the result derived by Buttiker *et.al.*[54] and Kramer[55], for the escape rate for the underdamped case. It was derived for our system in the case of titled washboard potential(The effective potential when one also considers the effect of non-conservative force) with $L = 2\pi$, given by

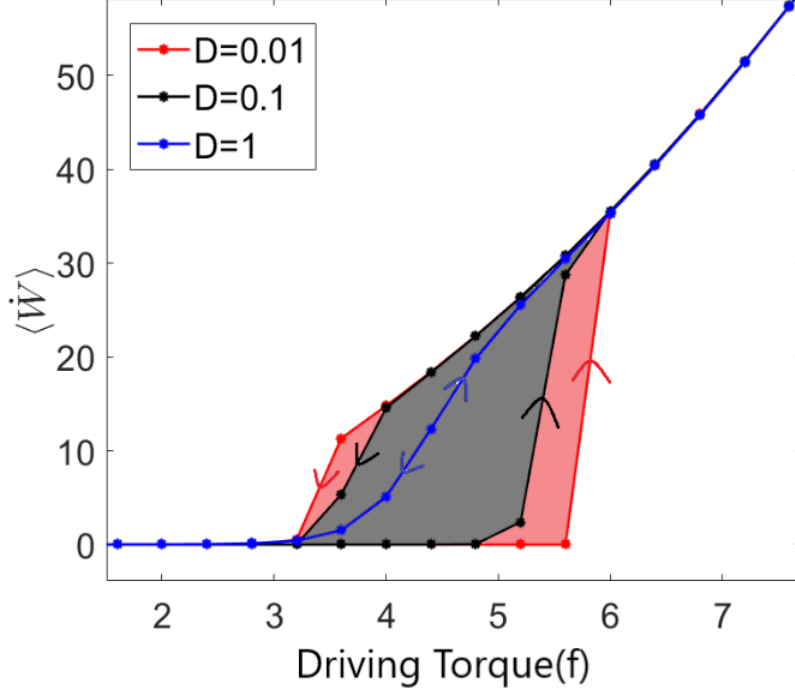$$\phi_{\text{eff}} = -\frac{f}{\gamma}x - \frac{k}{\gamma}\cos\left(x\right). \tag{2.53}$$

Figure 2.8: Hysteresis curve for average power for the underdamped system at $t = 10^5, k = 6, \gamma = 1$ for different temperatures. The arrow correspond to the direction of the change of driving force. We see that the area under the hysteresis curve decreases with increasing temperatures

The mean Kramer's escape time for extremely low damping ($G = \frac{\gamma}{\sqrt{kI}} \ll 1$) derived by Buttiker *et.al.* can be then computed as follows as,

$$\langle \tau_e \rangle = \frac{2\pi}{\omega_A} \exp\left(\frac{E_b}{k_B T}\right) \frac{[1 + (4\alpha DI/I_b)]^{1/2} + 1}{[1 + (4\alpha DI/I_b)]^{1/2} - 1} \left[\frac{I_b}{DI}\right] \tag{2.54}$$

where $\omega_A = |\omega_b| = \left(\frac{k}{I}\right)^{1/2} \left(1 - f^2/k^2\right)^{1/4}$ is the frequency associated to motion of the particle at the bottom/top of the well, E_b is the effective barrier height from well minimum, I_b is the action at the barrier peak and α is a fitting parameter relating to particle current at the barrier peak which is of order unity. Similarly, the Kramer's escape time for moderate damping ($G \sim O(1)$) derived by Kramer in 1940, is given by

$$\langle \tau_e \rangle = \frac{2\pi |\omega_b|}{\omega_A} \exp\left(\frac{E_b}{k_B T}\right) \frac{1}{\left[\left(\frac{\gamma^2}{4I^2} + |\omega_b|^2\right)^{1/2} - \frac{\gamma}{2I}\right]} \tag{2.55}$$

43

In Fig. (2.9), we show $\log_{10}(\langle\tau_e\rangle)$ as a function of driving torque in the bistable region. We find that for the parameter values used for the simulations in Fig. (2.8), the escape time, computed from the Kramer's formula Eqn. (2.54), is very high (increasing with increasing values of Eb, which goes from finite value $< 2k$ to 0 with increasing value of f). Since such a similar behaviour is seen when decreasing the driving torque from above, we expect the Kramer's escape time from limit cycle to stable node to be very high too.
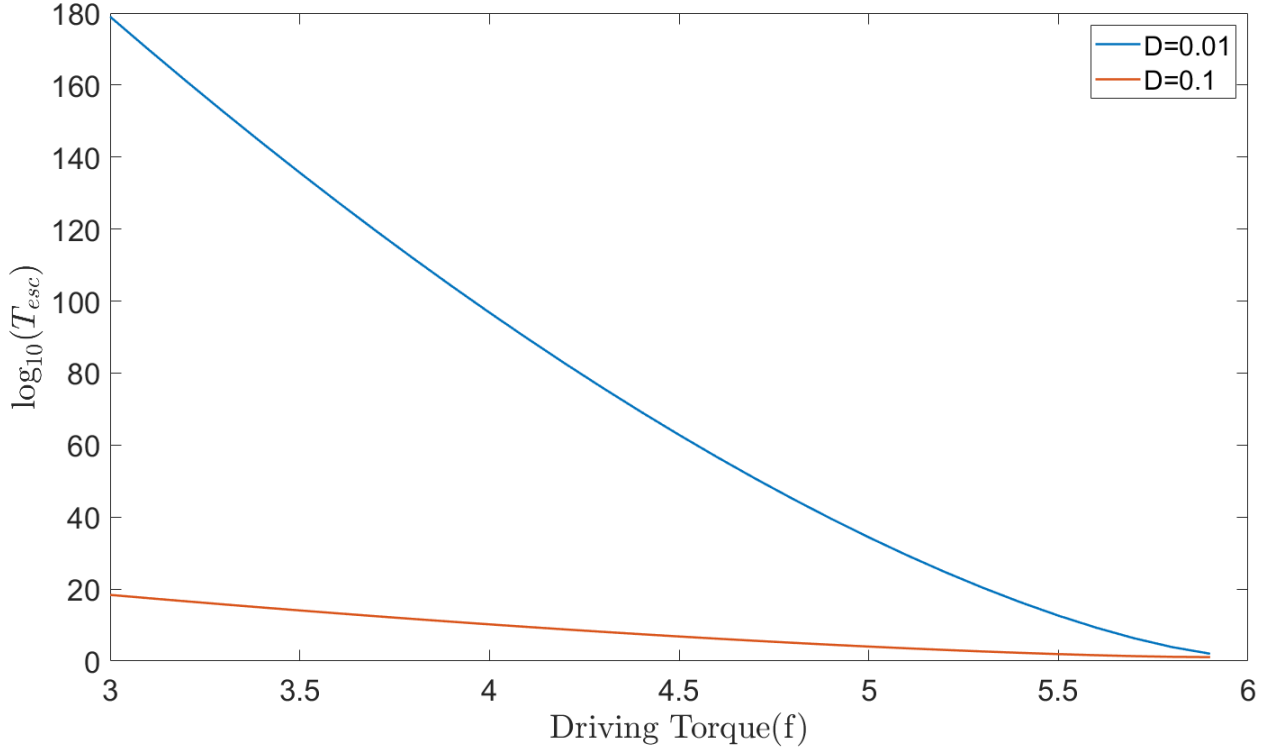

Figure 2.9: $\log_{10}(\langle\tau_e\rangle)$ vs Driving torque(f) in the bi-stable region for $k = 6, I = 1, \gamma = 1$. High values of Kramer's escape time corresponds to high stability of the potential well.

To utilize the effect of the meta-stability in the system, we also did numerical studies on the above system with external periodic driving in addition to constant external torque. The Langevin equation for the corresponding system is given by

$$I\ddot{\theta}_t + \gamma\dot{\theta}_t = \underbrace{f_0 + a\sin\left(\frac{2\pi t}{T_0}\right)}_{f_{\text{per}}(t)} - k\sin\left(\frac{2\pi\theta_t}{L}\right) + \eta(t) \tag{2.56}$$

44

where a and T_0 is the amplitude and time period of the driving respectively. f_0 and a is chosen such that it covers the entire bistable region and T_0 is such that it is lower than the Kramer's escape time from the well around f_0.
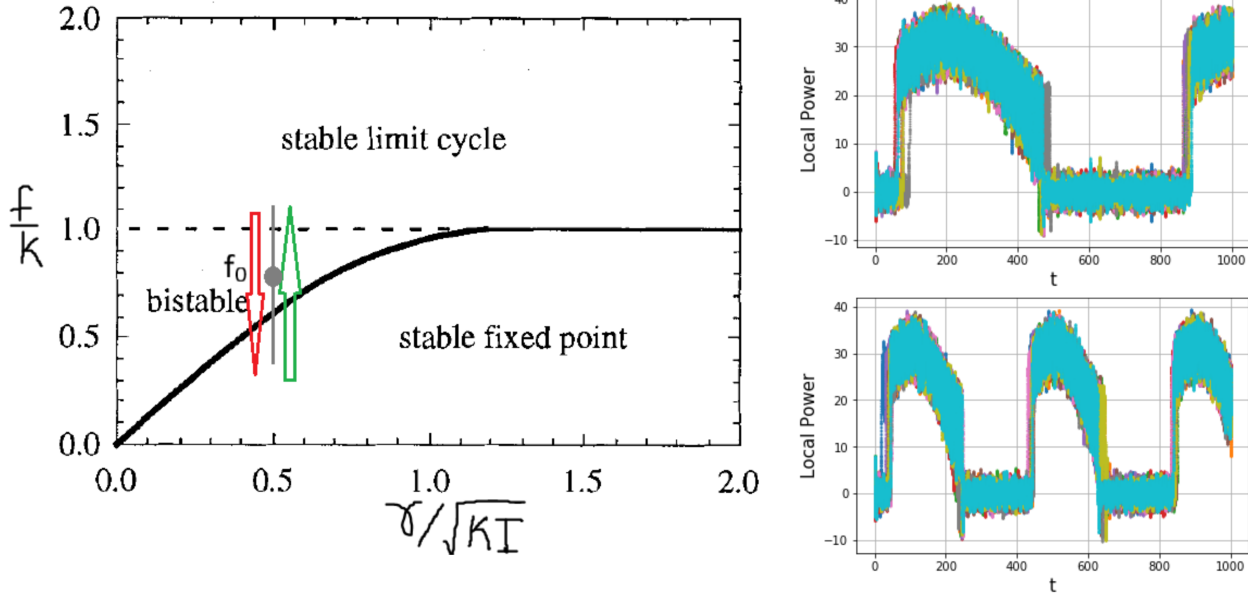

Figure 2.10: Left: Periodic driving in the Adler dynamics for the underdamped case in the bistable region. Right: Trajectories(10 samples) for system with time period,$T_0 = 800$(up) and $T_0 = 400$(down) .Parameters values: I=1, γ=1, f_0=4.5,k=6, $k_B T$=0.1, a=2.5.

The trajectories for the above system has clear structure which depends on the value of $G = \gamma/\sqrt{kI}$, f_0 and a and it seems independent of the time period of driving, T_0. Since, we began the protocol with initial conditions for the system to be in the basin of attraction of the stable node, the average power is almost 0, then suddenly spikes to the limit cycle solution(corresponding to the saddle-node bifurcation), then increases due to further increase of external torque.Now in the reverse protocol, the system stays in the limit cycle solution even in the bistable region, until the homoclinic bifurcation.

We also computed the average work inputted into the system in a cycle(over a single time period) and found a linear relationship with time period,T_0(shown below). This means the specific structure of the trajectories only gets rescaled with time period on average.
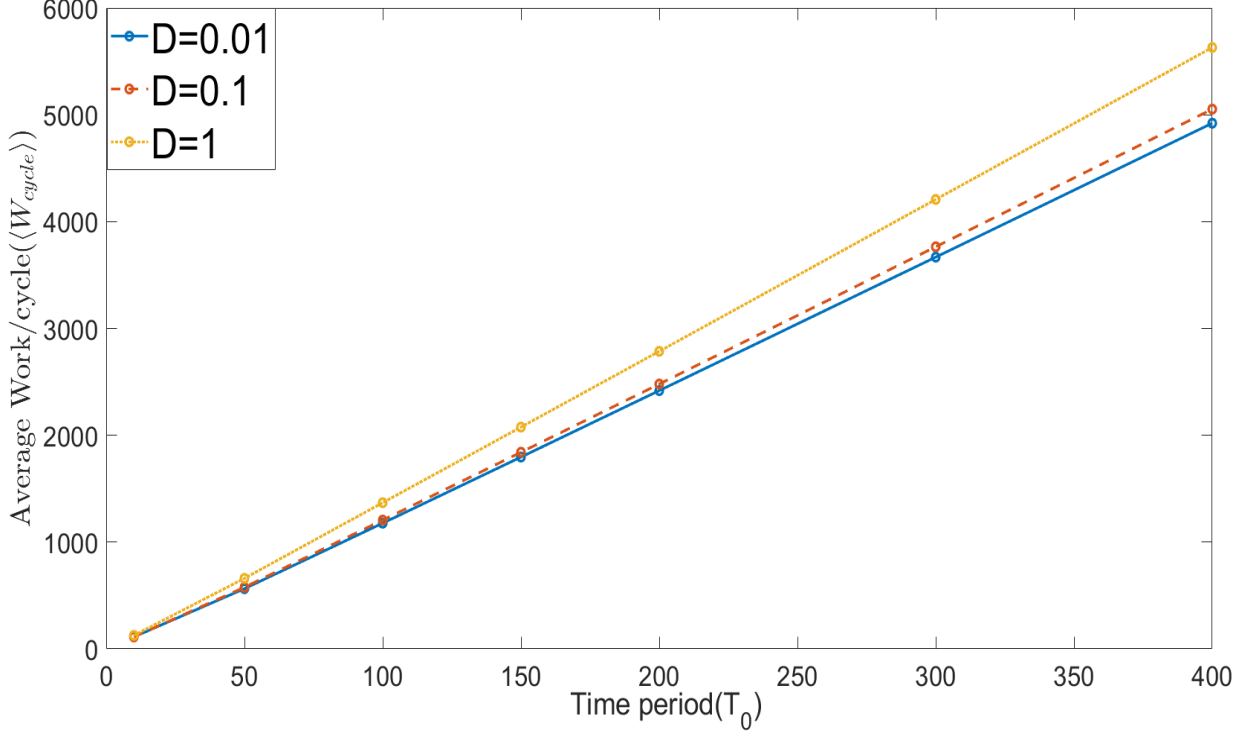
Figure 2.11: Average work inputted into the system per cycle vs time period of the driving for $k = 6, f_0 = 4.5, I = 1, \gamma = 1$ for different values of D. It shows a linear relationship between them, which implies the structure of the instantaneous power only gets rescaled with time period.The lines corresponds to the linear fit with goodness of fit, R^2=0.999

2.3 Nonlinear stochastic driven oscillator in an active bath

How does the non-equilibrium properties of the activity affect the thermodynamic quantities near the bifurcation behavior of non-linear system? To answer this question, we study the non-linear oscillator, the Adler oscillator, in the presence of active bath. In this section we will discuss only the overdamped limit of the dynamics and the corresponding equations of motion is given by

$$\dot{\theta}_t = \quad \frac{f}{\gamma} - \frac{k}{\gamma} \sin\left(\frac{2\pi\theta_t}{L}\right) + \xi_t \tag{2.57}$$

$$\langle \xi_t \rangle = 0, \langle \xi_t \xi_{t'} \rangle \quad = \frac{D}{\tau} \exp\left[-\frac{|t-t'|}{\tau}\right] \tag{2.58}$$

46

where we will define $D = \frac{k_B T}{\gamma}$ (effective diffusion coefficient due to the bath).So, effective strength of the active fluctuations at finite correlation time i given by $\langle \xi_t^2 \rangle = \frac{D}{\tau}$. Hence with correlation, one expects a cooling effect (decrease in the "effective" temperature, $T_{eff} = \frac{\gamma D}{k_B \tau}$) with correlation time. But one must remember that the exponential correlation also plays a key role, in controlling the different time scales in the system. As discussed in the above section, increasing the correlation time τ from $0 \to \infty$, corresponds to go from thermal bath limit to deterministic limit(i.e. infinitely correlated). Another interesting consequence of this system is that steady state average power inputted into the system is equal to the average heat dissipated in the active bath, i.e. $\langle \dot{W} \rangle = -\langle \dot{Q} \rangle$. This is due the bounded nature of the conservative potential,$\phi(\theta) = -\frac{2\pi k}{L} \cos\left(\frac{2\pi\theta}{L}\right)$.

To tackle the statistics of this model given by Eqn. (2.57), a non-Markovian problem, an effective Markovian problem can be constructed by adding extra degrees to capture the non-Markovian behaviour. The same statistics of the active fluctuations can be captured by modelling it as an Ornstein-Ulhenbeck process, given by

$$\tau \dot{\xi}_t = -\xi_t + \sqrt{2D}\eta_t \tag{2.59}$$

where η_t is white noise with zero mean and unit variance. Thus the Markovian representation of the original problem is 2-dimensional Langevin equation.

Taking the derivative of Eqn. (2.57), we can also describe the above system as an effective underdamped problem with space dependent friction,$\gamma(x; \tau)$ (See. Sec. 1.3.4), given by

$$\ddot{\theta}_t + \left[\tau^{-1} + \frac{2\pi k}{\gamma L} \cos\left(\frac{2\pi\theta_t}{L}\right)\right] \dot{\theta}_t = \frac{f - k\sin\left(\frac{2\pi\theta_t}{L}\right)}{\gamma\tau} + \frac{\sqrt{2D}}{\tau}\eta_t \tag{2.60}$$

After rescaling time, $\tilde{t} = t\tau^{-1/2}$, we obtain,

$$\ddot{\theta}_t + \left[\tau^{-1/2} + \tau^{1/2}\frac{2\pi k}{\gamma L} \cos\left(\frac{2\pi\theta_t}{L}\right)\right] \dot{\theta}_t = \frac{f - k\sin\left(\frac{2\pi\theta_t}{L}\right)}{\gamma} + \frac{\sqrt{2D}}{\tau^{1/4}}\eta_t \tag{2.61}$$

where the space dependent friction, $\gamma_{\text{eff}}(\theta, \tau) = \tau^{-1/2} + \tau^{1/2}\left(\frac{2\pi k}{\gamma L}\right)\cos\left(\frac{2\pi\theta_t}{L}\right)$. One may notice that as correlation time,τ increases (when $\tau > \frac{\gamma L}{2\pi k}$, the friction is also negative(i.e. accelerating) for some values of the phase space ($\theta \in [\pi/2, 3\pi/2]$ at $\tau \to \infty$). The negative friction is essential for the spontaneous oscillations seen in hair bundle systems[56]
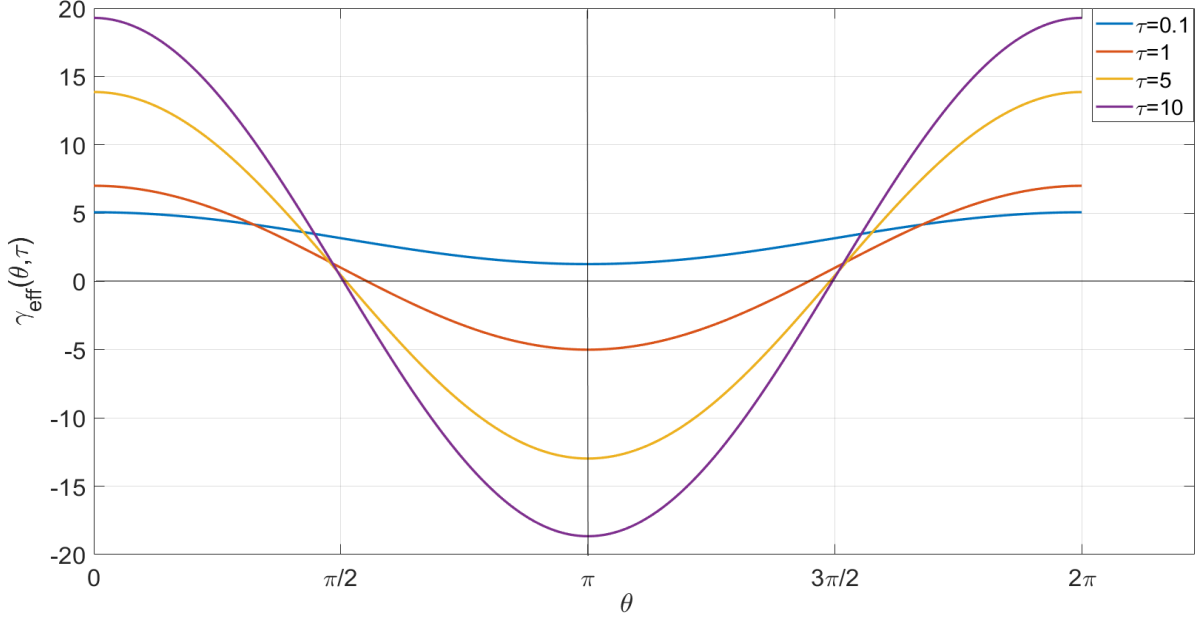
47

Figure 2.12: Space dependent friction as function of θ for different correlation times. Parameters: $k=6, L = 2\pi, \gamma = 1$. One can see that for larger correlation times the friction is negative for a part of the phase space.

First I will discuss the two approximation schemes, Fox's approximation and UCNA, which has previously been successfully used to describe the equilibrium system for small correlation time (i.e. $\sqrt{D\tau} < l_0$, where l_0 is the characteristic length of the system). We would like to check the validity of these approximations to our driven non-linear system. The Fokker-Plank equation for the Fox's approximation for our model is given by

$$\frac{\partial P(\theta, t)}{\partial t} = -\frac{1}{\gamma}\frac{\partial}{\partial \theta}\left[\left\{f - k\sin\left(\frac{2\pi\theta}{L}\right)\right\}P(\theta, t)\right] + D\frac{\partial^2}{\partial \theta^2}\frac{P(\theta, t)}{\left(1 + \frac{2\pi k\tau}{L}\cos\left(\frac{2\pi\theta}{L}\right)\right)} \quad (2.62)$$

In the steady state, one finds that the distribution can be computed during similar manipulations to Sec. 2.2 ,

$$P_{\text{st}}^f(\theta) = \frac{1}{N_{\text{fox}}}\exp\{-V(\theta)\}\int_{\theta}^{\theta+L} d\theta' \exp\{V(\theta')\}\left[1 + \frac{2\pi k\tau}{L}\cos\left(\frac{2\pi\theta'}{L}\right)\right] \quad (2.63)$$

48

where,

$$V(\theta) \equiv \quad \frac{1}{DL}\left[\frac{-fL\theta}{\gamma} + \frac{kL^2}{2\pi\gamma}\cos\left(\frac{2\pi\theta}{L}\right) - \frac{k^2L\tau}{4\gamma^2}\cos\left(\frac{4\pi\theta}{L}\right) - \frac{fkL\tau}{\gamma^2}\sin\left(\frac{2\pi\theta}{L}\right)\right]$$
$$- \log\left[1 + \frac{2\pi k\tau}{\gamma L}\cos\left(\frac{2\pi\theta}{L}\right)\right].$$

The first term is equivalent to the potential of the system for the steady state problem in the Markovian regime. Given the probability distribution, the average power inputted into the system in the steady state can be computed similar to Sec. 2.2.1, given by

$$\langle \dot{W}_{\text{fox}} \rangle = \frac{fDL}{N_{\text{fox}}}(1 - \exp[fL/\gamma D]) \tag{2.64}$$

Similarly, for UCNA, the Fokker-Planck equation is given by

$$\frac{\partial P(\theta,t)}{\partial t} = -\frac{\partial}{\partial\theta}\left[\frac{\left\{f - k\sin\left(\frac{2\pi\theta}{L}\right)\right\}P(\theta,t)}{1 + \frac{2\pi k\tau}{L}\cos\left(\frac{2\pi\theta}{L}\right)}\right] + D\frac{\partial}{\partial\theta}\frac{1}{\left[1 + \frac{2\pi k\tau}{L}\cos\left(\frac{2\pi\theta}{L}\right)\right]}\frac{\partial}{\partial\theta}\frac{P(\theta,t)}{\left[1 + \frac{2\pi k\tau}{L}\cos\left(\frac{2\pi\theta}{L}\right)\right]}$$

$$\tag{2.65}$$

The stationary distribution, is given by

$$P_{st}^{U}(\theta) = \frac{1}{N_{\text{UCNA}}}\exp\{-V(\theta)\}\int_{\theta}^{\theta+L}d\theta'\exp\{V(\theta')\}\left[1 + \frac{2\pi k\tau}{L}\cos\left(\frac{2\pi\theta'}{L}\right)\right]^2 \tag{2.66}$$

So the only difference between these two approximations in the steady state is the extra factor, $\left[1 + \frac{2\pi k\tau}{L}\cos\left(\frac{2\pi\theta'}{L}\right)\right]$ (space dependent friction), which wouldn't have mattered in the equilibrium case. The average power inputted into the system in the steady state according to UCNA, is given by

$$\langle \dot{W}_{\text{UCNA}} \rangle = \frac{fDL}{N_{\text{UCNA}}}(1 - \exp[fL/\gamma D]) \tag{2.67}$$

The key quantity needed to evaluate the average steady state power is the normalization constant, $N_{\text{fox}} = \int_0^L d\theta P_{\text{st}}^f(\theta)$ and $N_{\text{UCNA}} = \int_0^L d\theta P_{\text{st}}^U(\theta)$. The above quantities are further evaluated by numerical integration of the above normalization condition. It must noted that both N_{fox} and N_{UCNA} are dependent on all the system parameters.

Both these approximations are only valid in the entire phase space, only when the space dependent diffusivity and friction are positive. This imposes another restriction on the

49

correlation time, $1 + \frac{2\pi k\tau}{L} \cos\left(\frac{2\pi\theta}{L}\right) > 0$,i.e., $\tau < \frac{\gamma L}{2\pi k}$, in addition to the convergence issues for large τ. We first compared both the distributions for correlation times when these approximations are physical with the distribution obtained from the simulations. One notices that there is significant deviation in the stationary distribution obtained from
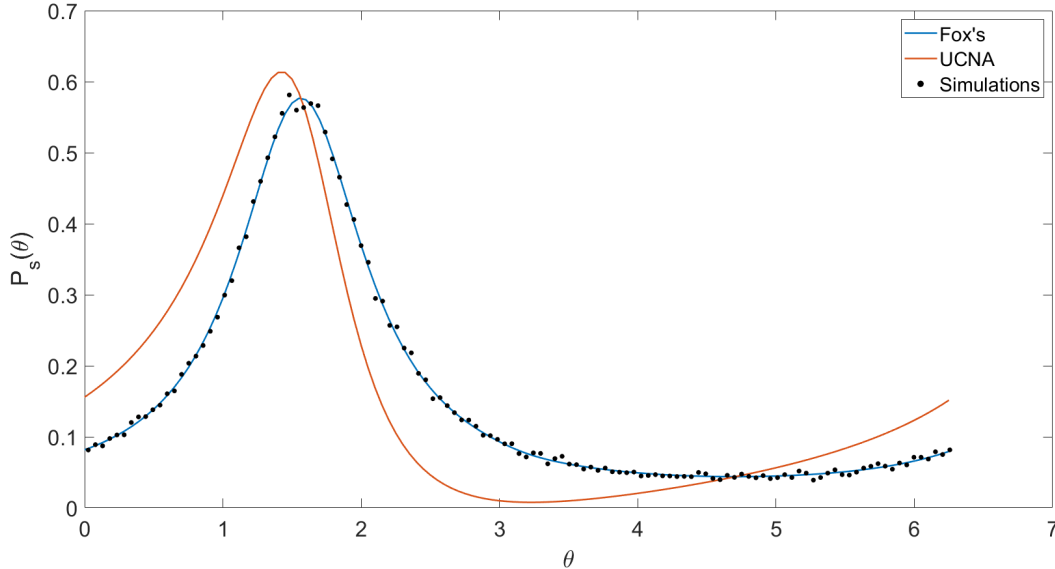

Figure 2.13: Stationary distribution, $P_s(\theta)$ for $f = 7, k = 6, D = 0.01$ and $\gamma = 1$

UCNA compared to the simulations, whereas the "Fox's" approximation converges . UCNA fails for this model due to the presence of driving torque, which drives the system out of equilibrium(lack of detailed balance) independent of the noise. Whereas, Fox's approximation can be still derived independent of the detailed balance condition[57]. We will show below that even Fox's approximation's validity is limited to parameter values where the velocity distribution is close to Gaussian. So, for small correlation times, where the system soon looses the memory of initial velocity and reaches a stationary distribution, which is close to Gaussian. From the Chapman-Enskog calculation, we can show that the angular velocity distribution takes the form of product of Gaussian and a polynomial in τ (See Appendix C). This implies there is further deviation from the Gaussian as one increases the correlation time and deviations are also dependent on parameter values of the problem. Below, we will show an example of this non-Gaussian behaviour, where even for small correlation times, the Fox's approximation does not capture the stationary distribution very well and one can relate the cause to the velocity distributions.
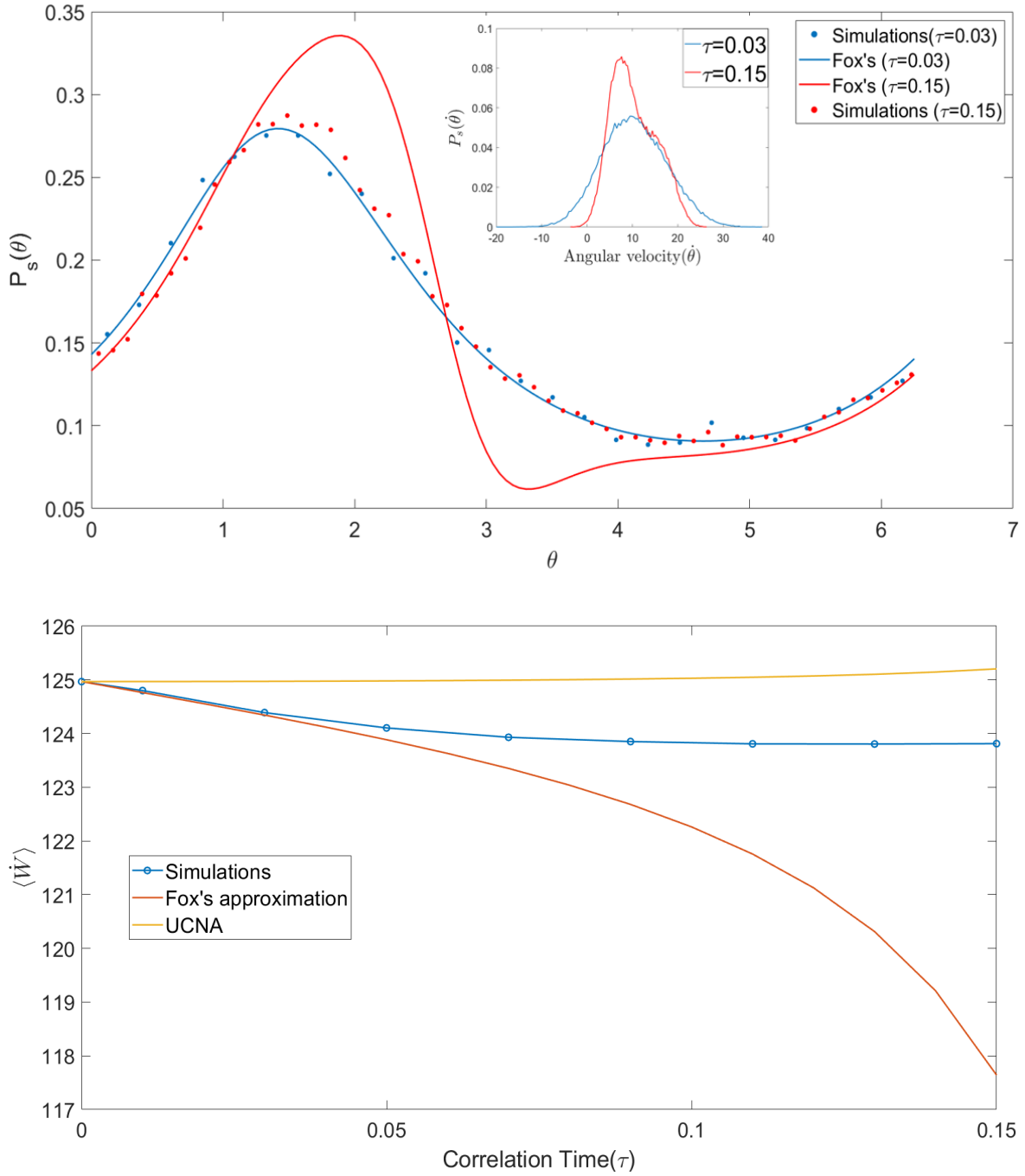
Figure 2.14: Up: Stationary distribution for the phase, $P_s(\theta)$ for different values of τ, when $f = 12, k = 6, \gamma = 1, D = 1$ from simulations along with Fox's approximation. One can see that for $\tau = 0.15$, Fox's approximation deviated a lot from the simulations. Down: Stationary distribution for the velocity,$P_s\dot{\theta}$ for the same parameter values. One can see that for $\tau = 0.15$, the velocity distribution deviates from the Gaussian.

We then looked at the average power inputted into the system in the steady state for different correlation times. Since the average power for the thermal bath case is always more than the deterministic case, we expect the average power to decrease from the thermal bath limit to the deterministic limit as one increases the activity,τ, from $0 \to \infty$. We have also compared the results of the simulations with power computed from Fox's approximation (Eqn. (2.64)), for small correlation times, where the approximation is valid. But, numerically
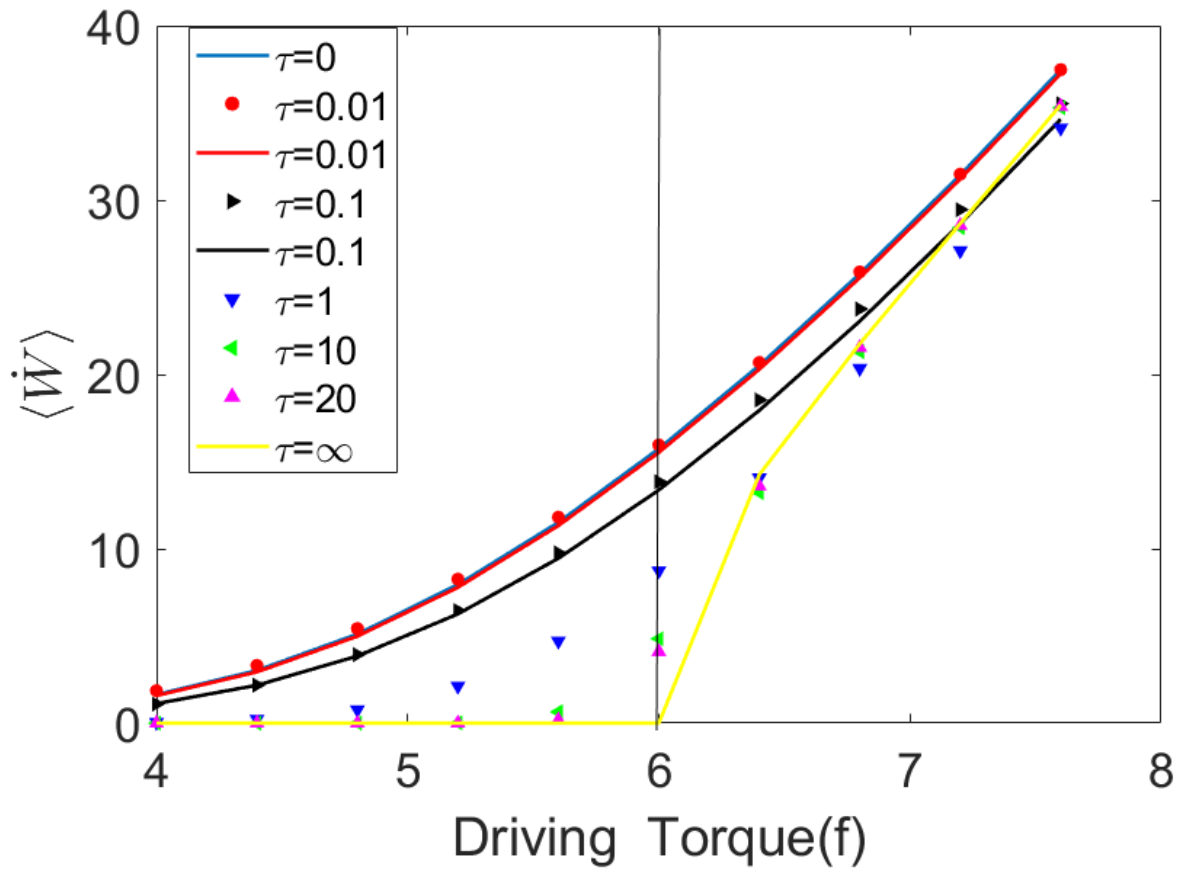

Figure 2.15: Average power with driving torque(f) for $D = 1, k = 6$ for different correlation times. Here the lines correspond to the average power(Eqn(!)) obtained from Fox's approximation(here only valid for $\tau < 1/6$). We can see that with increasing τ corresponds to going from thermal bath limit $(\tau = 0)$ to the deterministic case$(\tau = \infty)$.

we observed that there is a distinction in the behaviour of average power inputted into the system, for values of external driving torque, f, below and above the bifurcation point $(f = k)$. The average power below the bifurcation, behaves in the way we expect where

52

increasing correlation, decreases the effective temperature of the bath, $T_{eff} = \frac{\gamma D}{k_B \tau}$. We know from the thermal bath case that decreasing temperature, decreases the average power and finally converging to the deterministic case ($\langle \dot{W} \rangle = 0$). So below the bifurcation point, the increasing the correlation time of the bath, corresponds to effective cooling of the system. Whereas, above the bifurcation point, where the deterministic case has running state (See Sec. 2.2.1), the correlation time has more interesting implications (See Fig. 2.16(b)).
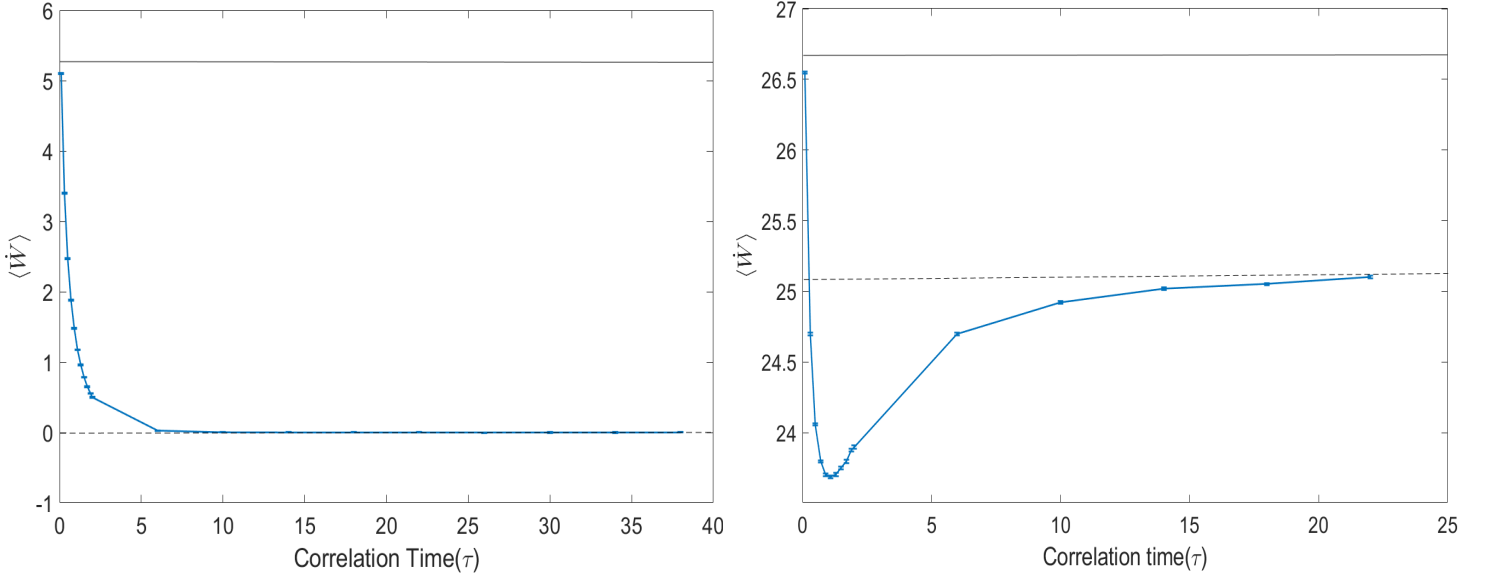

Figure 2.16: Average power in the steady state vs correlation time(τ), when $k = 6, D = 1, \gamma = 1, Ł = 2\pi$ for values of external torque ,below the bifurcation point, $f = 5$,(Left) and above the bifurcation point, $f = 7$ (Right). τ_c corresponds to correlation time when the system has minimum power. Dashed Horizontal line corresponds to the deterministic case and Dotted line corresponds to the Thermal bath case with same parameters.

As we can see, the average power inputted into the system has a non-monotonous behaviour with correlation time,τ, above the bifurcation point($f = k$). One key observation is that the average power can go below the value in deterministic limit, which was not possible for any finite temperature in the thermal bath limit. There also exists a critical correlation time, τ_c, where the average power in minimum, i.e. the rate of dissipation of heat into the bath at τ_c is minimum. So, for small activity of the bath ($\tau < \tau_c$), it has a cooling effect on the system, whereas it has an heating for $\tau \geq \tau_c$. We believe such a non-monotonous behaviour above the bifurcation point, is a combination of effect of persistence in the running state and also the cooling effect of the active bath, $D_{eff} = \frac{D}{\tau}$.Even though,

stationary distribution of phase doesn't show any clear change with correlation time, we find that the above behaviour is well captured in the stationary distribution of the angular velocity(Fig. 2.17). We can see that the angular velocity where the first peak occurs shows such a non-monotonous behaviour. The presence of second peak in the velocity distribution with correlation time corresponds to the peak in the velocity distribution(averaged over phase distribution) in the deterministic case, $P_{\text{det}}(\dot{\theta} = v) \propto \frac{1}{v\sqrt{k^2-(f-\gamma v)^2}}$, where the variation in the velocity is minimum. One can observe that the velocity distributions are in general non-Gaussian(Fig. 2.17), even at small correlation times, implying that even Fox's approximation wouldn't be able to capture this non-monotonous behaviour. We predict such a behaviour in any non-linear driven systems(1-dimensional) under the effect of active fluctuations.
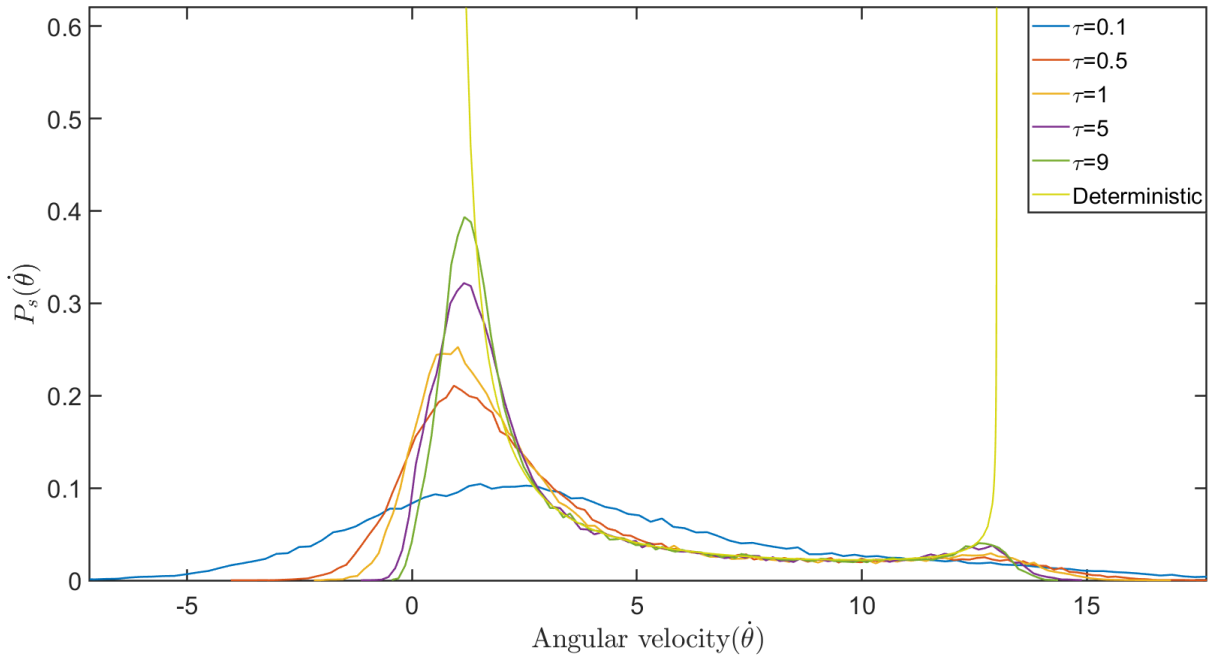

Figure 2.17: Stationary distribution of angular velocity, $\dot{\theta}$ for different correlation times, when $f = 7, k = 6, D = 1, \gamma = 1, L = 2\pi$

We also investigated the effect of increasing the period of the non-linear potential, L. We expect that for very large $L \gg 1$, the system will behave similar to drift-diffusion problem. We plot below the above plot of average power for different periods. We can see that average power seems to become constant independent of correlation times,τ, for larger L. This is due to the fact that for drift diffusion process, the average velocity, $\langle\dot{\theta}\rangle$ is independent of the form of correlation function of the noise, $\Gamma(t - t')$.
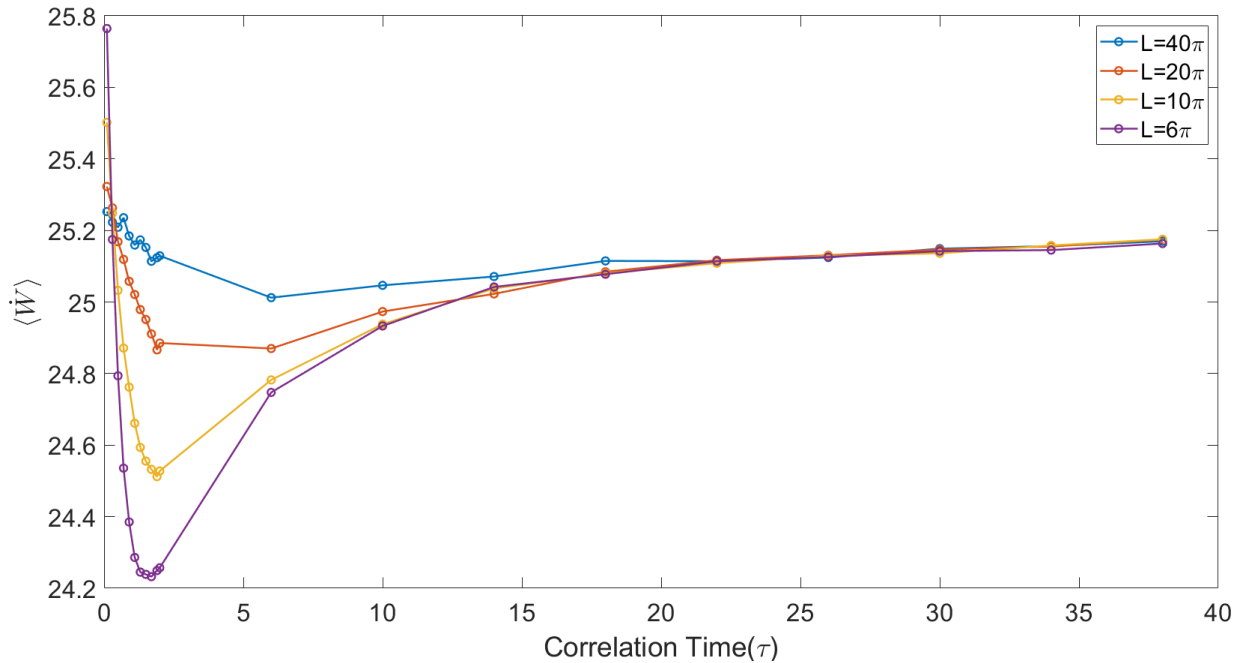
54

Figure 2.18: Average power with correlation time τ for $D = 1, k = 6, f = 7, \gamma = 1$ for different periods of the potential.

First passage properties has been successfully used to produce lower bounds for the estimation of entropy production in the system[31]. In the active bath case, the entropy production has contributions from both the dissipation and non-equilibrium nature of the bath, therefore the bounds cannot be directly related to the dissipation in the system. But in the thermal bath case, one can find equalities relating moments of first passage and moments of integrated current[53]. We found that one can use first passage properties to find lower bounds for the average power inputted into the system. Let us define, $\langle \mathcal{T}(A) \rangle$ as the mean first passage time to be absorbed in any of the two symmetric absorbing boundaries at, $x = \pm A$, where x is the real line extension of the phase($\theta = x \mod (2\pi)$) such that $\mathcal{T}(A) \equiv \inf\{t \geq 0 / x(t) \notin [-A, A], x(0) = 0\}$. We can then define a lower bound for the power inputted into the system, given by

$$\langle \dot{W} \rangle \geq \frac{fA}{\langle \mathcal{T}(A) \rangle} \tag{2.68}$$

We see that the bound is sensitive to whether $A = 2n\pi$ or $A = (2n + 1)\pi$, with better bounds achieved for $A = 2n\pi$(where n is a positive integer). As expected, the bound is
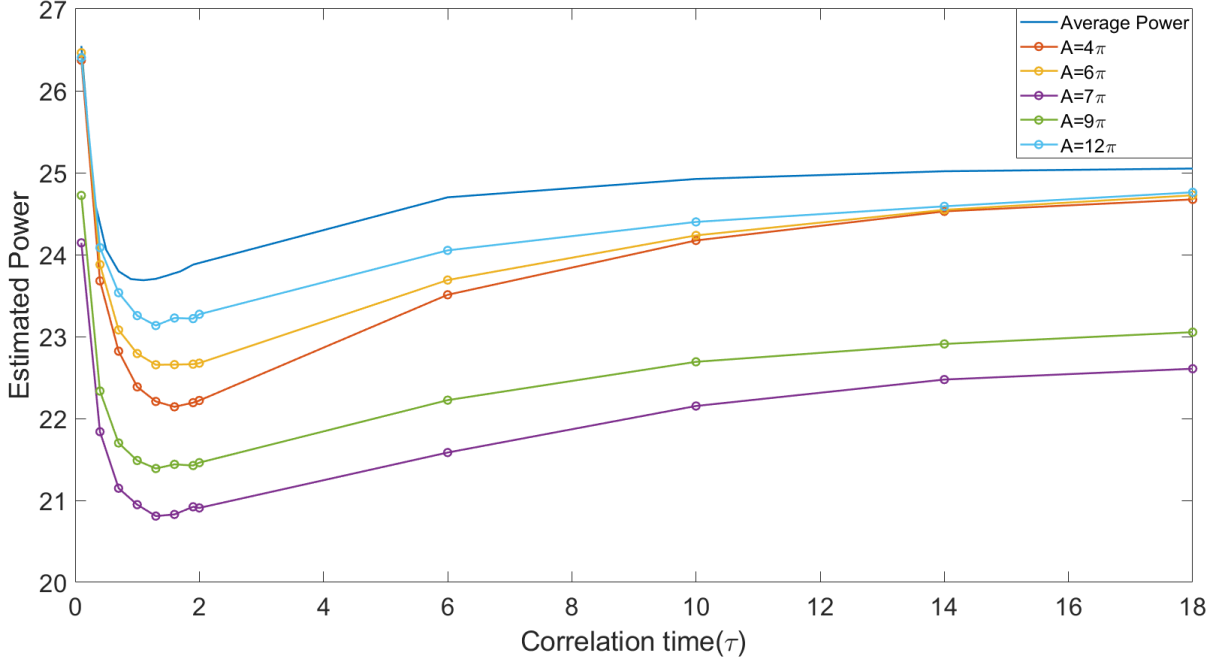
55

Figure 2.19: Estimated average power with correlation time τ for $D = 1, k = 6, f = 7, \gamma = 1$ for different lengths for the boundary of the absorbing wall, A. The plot with no markers correspond to the average power obtained from the simulations whereas the ones with marker are the estimated power using Eqn. (2.68).

better for larger values of A, as there are fewer particles going against the external torque and the mean first passage converges to the mean time period for the system.

We also looked at the variance in the work inputted into the system, $\sigma^2_{W_t}$ at large times in the steady state for different correlation times. In the thermal bath limit($\tau \to 0$), the variance in work had a peak at the bifurcation point. With the increase in correlation time, we found out that the variance in work done is further enhanced at the bifurcation point, whereas the peak as function of external torque around the bifurcation point, sharpens with correlation time. For correlation time $\tau \to \infty$, we reach the deterministic limit, where the variance is zero for all values of external torque, except the bifurcation point. The increase in variance at the bifurcation point with correlation time can be explained through the effect of persistence(even though the strength decreases with τ).At the bifurcation point, which is highly unstable, the persistence for values of $\xi > 0$ plays a positive role in enhancing the displacement in the running state whereas when the persistence for values of $\xi < 0$, just falls into fixed point where variance is just governed by the strength of the noise(which

vanishes with increasing τ). Since, the variance in work(at large times) is also related the effective diffusion constant, as shown in Sec. 2.2.1, the diffusion can be further enhanced at the bifurcation point with increasing correlation time.
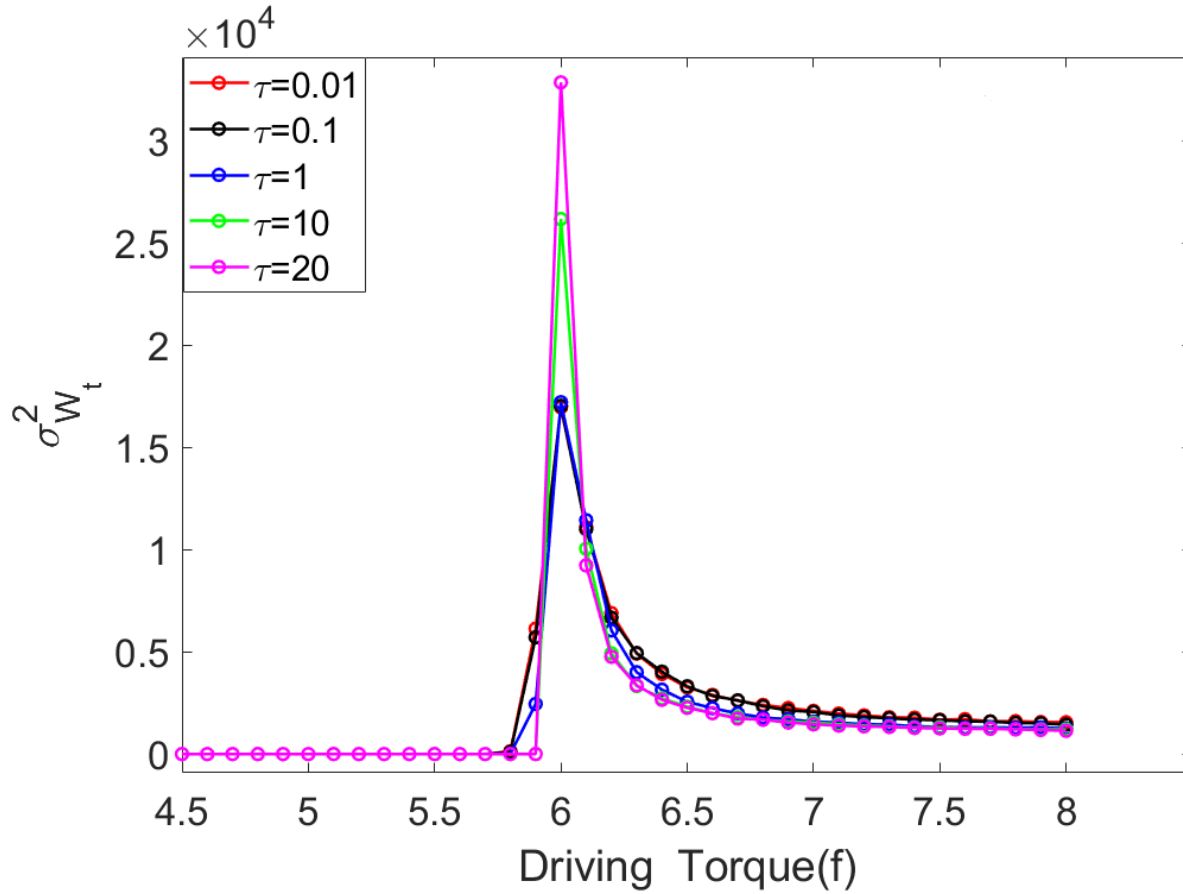

Figure 2.20: Variance in work inputted into the system in steady state for different correlation time τ with $D = 0.01, k = 6, \gamma = 1$ at t=400.

Chapter 3

Conclusions & Outlook

In this thesis, we have studied the statistics of thermodynamic quantities for a non-linear oscillator in the presence of different baths, thermal and active baths, at the non-equilibrium steady state using the framework of stochastic thermodynamics.Noise induced effects on the thermodynamic quantities near the bifurcation point and the effects of active fluctuations in the system were explored.

In the presence of thermal bath, we have derived analytical expressions for the average power and variance in the work inputted into the system in the overdamped limit. We found out that the presence of a thermal bath enhances the power inputted into the system and it also follows a scaling law with temperature of the bath, $\langle \dot{W} \rangle \propto T^{1/3}$ at the bifurcation point. The variance of the work inputted into the system shows a peak at the bifurcation point for low temperatures. So, for precise enhancement of power inputted into the system, one must stay above the bifurcation point. Numerical studies on the underdamped limit in the presence of thermal bath, suggests that the system takes significant time to relax to unique steady state in the region of bistability. The signatures of metastability can be observed in the thermodynamic quantities through hysteresis effects and the relaxation times to the steady states has been estimated using Kramer's escape rate analysis. One can also utilize the metastability to design asymmetric input of power into the system, using symmetric periodic driving the system, even in the presence of the bath.

In the presence of active bath, the system has much richer phenomenology due to the non-equilibrium nature of the bath. An extensive study of two different approximations-

Fox's approximation and Unified color noise approximation (UCNA), used to study the ensemble properties in the presence of active fluctuations was also conducted. We found that UCNA doesn't capture the steady state properties for any correlation time, whereas Fox's approximation is limited to correlation times until the velocity distributions are close to Gaussian form. Controlling the correlation time(activity) of the bath, one finds that the behaviour of the system goes from the one in presence of thermal bath to deterministic case (absence of bath). Numerical studies of the average power in the steady state suggest that above the bifurcation point, the activity has both cooling and heating effect on the system and there is finite critical correlation time when the system dissipates the minimum. The average power at the critical correlation time, τ_c, can also go below the deterministic case, which is not possible for the thermal bath. The study on the different approximations suggests that one must look at the higher order terms in correlation to capture the non-monotonous behaviour in the power. The existence of minimum average power at finite correlation time, is reminiscent of stalling forces in Brownian motors. We also found that the diffusive behaviour can be much more enhanced at the bifurcation point for low temperatures as compared to thermal bath case, by increasing the correlation time. The variance in the work inputted also shows a peak at the bifurcation point which becomes sharper and higher with correlation time.

The above study of effects of active fluctuations on driven non-linear systems opens new theoretical avenues. Better Markovian approximations need to be developed for the analytical study of the behaviour near critical correlation time, τ_c, to capture the higher order currents. The above study also calls for experimental study for power regulation using correlations in noise in Josephson junctions, power grids , hair bundles etc. Here, we have looked only at the effect of active fluctuation for a single oscillator. It will also be really interesting to study the influence of active fluctuations in coupled oscillators, particularly in the phenomenon of synchronization.

Bibliography

[1] Richard J Field. *Oscillations and traveling waves in chemical systems*. Wiley, 1985.

[2] Deepak Dhar. Theoretical studies of self-organized criticality. *Physica A: Statistical Mechanics and its Applications*, 369(1):29–70, 2006.

[3] Thierry Mora and William Bialek. Are biological systems poised at criticality? *Journal of Statistical Physics*, 144(2):268–302, 2011.

[4] Roberto Di Leonardo, Luca Angelani, D Dell'Arciprete, Giancarlo Ruocco, Valerio Iebba, Serena Schippa, Maria Pia Conte, F Mecarini, F De Angelis, and E Di Fabrizio. Bacterial ratchet motors. *Proceedings of the National Academy of Sciences*, 107(21):9541–9545, 2010.

[5] Eamonn A Gaffney, H Gadêlha, DJ Smith, JR Blake, and JC Kirkman-Brown. Mammalian sperm motility: observation and theory. *Annual Review of Fluid Mechanics*, 43:501–528, 2011.

[6] Howard C Berg. *E. coli in Motion*. Springer Science & Business Media, 2008.

[7] Andreas Walther and Axel HE Müller. Janus particles. *Soft Matter*, 4(4):663–668, 2008.

[8] Michael E Cates. Diffusive transport without detailed balance in motile bacteria: does microbiology need statistical physics? *Reports on Progress in Physics*, 75(4):042601, 2012.

[9] Vijay Narayan, Sriram Ramaswamy, and Narayanan Menon. Long-lived giant number fluctuations in a swarming granular nematic. *Science*, 317(5834):105–108, 2007.

[10] Michael E Cates and Julien Tailleur. Motility-induced phase separation. *Annu. Rev. Condens. Matter Phys.*, 6(1):219–244, 2015.

[11] Nitin Kumar, Harsh Soni, Sriram Ramaswamy, and AK Sood. Flocking at a distance in active granular matter. *Nature communications*, 5(1):1–9, 2014.

[12] J Tailleur and ME Cates. Sedimentation, trapping, and rectification of dilute bacteria. *EPL (Europhysics Letters)*, 86(6):60002, 2009.

[13] Peter Galajda, Juan Keymer, Paul Chaikin, and Robert Austin. A wall of funnels concentrates swimming bacteria. *Journal of bacteriology*, 189(23):8704–8707, 2007.

[14] Sudeesh Krishnamurthy, Subho Ghosh, Dipankar Chatterji, Rajesh Ganapathy, and AK Sood. A micrometre-sized heat engine operating between bacterial reservoirs. *Nature Physics*, 12(12):1134–1138, 2016.

[15] Édgar Roldán, Jérémie Barral, Pascal Martin, Juan MR Parrondo, and Frank Jülicher. Arrow of time in active fluctuations. *arXiv preprint arXiv:1803.04743*, 2018.

[16] Nicolas Bruot and Pietro Cicuta. Realizing the physics of motile cilia synchronization with driven colloids. *Annual Review of Condensed Matter Physics*, 7:323–348, 2016.

[17] Hannes Risken. Fokker-planck equation. In *The Fokker-Planck Equation*, pages 63–95. Springer, 1996.

[18] Peter Reimann. Brownian motors: noisy transport far from equilibrium. *Physics reports*, 361(2-4):57–265, 2002.

[19] Björn Nadrowski, Pascal Martin, and Frank Jülicher. Active hair-bundle motility harnesses noise to operate near an optimum of mechanosensitivity. *Proceedings of the National Academy of Sciences*, 101(33):12195–12200, 2004.

[20] Roie Shlomovitz, Yuttana Roongthumskul, Seung Ji, Dolores Bozovic, and Robijn Bruinsma. Phase-locked spiking of inner ear hair cells and the driven noisy adler equation. *Interface focus*, 4(6):20140022, 2014.

[21] Shamik Gupta, Alessandro Campa, and Stefano Ruffo. *Statistical Physics of Synchronization*. Springer, 2018.

[22] Juan A Acebrón, Luis L Bonilla, Conrad J Pérez Vicente, Félix Ritort, and Renato Spigler. The kuramoto model: A simple paradigm for synchronization phenomena. *Reviews of modern physics*, 77(1):137, 2005.

[23] Ken Sekimoto. *Stochastic energetics*, volume 799. Springer, 2010.

[24] Udo Seifert. Stochastic thermodynamics, fluctuation theorems and molecular machines. *Reports on progress in physics*, 75(12):126001, 2012.

[25] Ignacio A Martínez, Édgar Roldán, Luis Dinis, and Raúl A Rica. Colloidal heat engines: a review. *Soft matter*, 13(1):22–36, 2017.

[26] Christopher Jarzynski. Equalities and inequalities: Irreversibility and the second law of thermodynamics at the nanoscale. *Annu. Rev. Condens. Matter Phys.*, 2(1):329–351, 2011.

[27] Stephen Strogatz. Nonlinear dynamics and chaos: with applications to physics, biology, chemistry, and engineering (studies in nonlinearity). 2001.

[28] Indrani Bose and Sayantari Ghosh. Bifurcation and criticality. *Journal of Statistical Mechanics: Theory and Experiment*, 2019(4):043403, 2019.

[29] Langevin dynamics. http://physics.gu.se/ frtbm/joomla/media/mydocs/LennartSjogren/kap6.pdf. Accessed: 2020-03-27.

[30] Andre C Barato and Udo Seifert. Thermodynamic uncertainty relation for biomolecular processes. *Physical review letters*, 114(15):158101, 2015.

[31] Édgar Roldán, Izaak Neri, Meik Dörpinghaus, Heinrich Meyr, and Frank Jülicher. Decision making in the arrow of time. *Physical review letters*, 115(25):250602, 2015.

[32] Jordan M Horowitz and Todd R Gingrich. Thermodynamic uncertainty relations constrain non-equilibrium fluctuations. *Nature Physics*, pages 1–6, 2019.

[33] Frank Moss and Peter VE McClintock. *Noise in nonlinear dynamical systems*, volume 2. Cambridge University Press, 1989.

[34] Peter Hänggi and Peter Jung. Colored noise in dynamical systems. *Advances in chemical physics*, 89:239–326, 1995.

[35] Claudio Maggi, Matteo Paoluzzi, Nicola Pellicciotta, Alessia Lepore, Luca Angelani, and Roberto Di Leonardo. Generalized energy equipartition in harmonic oscillators driven by active baths. *Physical review letters*, 113(23):238303, 2014.

[36] Aykut Argun, Ali-Reza Moradi, Erçağ Pinçe, Gokhan Baris Bagci, Alberto Imparato, and Giovanni Volpe. Non-boltzmann stationary distributions and nonequilibrium relations in active baths. *Physical Review E*, 94(6):062150, 2016.

[37] José M Sancho, M San Miguel, SL Katz, and JD Gunton. Analytical and numerical studies of multiplicative noise. *Physical Review A*, 26(3):1589, 1982.

[38] N Koumakis, C Maggi, and R Di Leonardo. Directed transport of active particles over asymmetric energy barriers. *Soft matter*, 10(31):5695–5701, 2014.

[39] LL Bonilla. Active ornstein-uhlenbeck particles. *Physical Review E*, 100(2):022601, 2019.

[40] Ronald F. Fox. Functional-calculus approach to stochastic differential equations. *Phys. Rev. A*, 33:467–476, Jan 1986.

[41] Ronald Forrest Fox. Uniform convergence to an effective fokker-planck equation for weakly colored noise. *Phys. Rev. A*, 34:4525–4527, Nov 1986.

[42] Jaume Masoliver, Bruce J. West, and Katja Lindenberg. Bistability driven by gaussian colored noise: First-passage times. *Phys. Rev. A*, 35:3086–3094, Apr 1987.

[43] Peter Jung and Peter Hänggi. Dynamical systems: A unified colored-noise approximation. *Phys. Rev. A*, 35:4464–4466, May 1987.

[44] F. Castro, H. S. Wio, and G. Abramson. Colored-noise problem: A markovian interpolation procedure. *Phys. Rev. E*, 52:159–164, Jul 1995.

[45] Lennart Dabelow, Stefano Bo, and Ralf Eichhorn. Irreversibility in active matter systems: Fluctuation theorem and mutual information. *Phys. Rev. X*, 9:021009, Apr 2019.

[46] Lorenzo Caprini, Umberto Marini Bettolo Marconi, Andrea Puglisi, and Angelo Vulpiani. The entropy production of ornstein–uhlenbeck active particles: a path integral method for correlations. *Journal of Statistical Mechanics: Theory and Experiment*, 2019(5):053203, may 2019.

[47] Étienne Fodor, Cesare Nardini, Michael E Cates, Julien Tailleur, Paolo Visco, and Frédéric van Wijland. How far from equilibrium is active matter? *Physical review letters*, 117(3):038103, 2016.

[48] Martin Rohden, Andreas Sorge, Marc Timme, and Dirk Witthaut. Self-organized synchronization in decentralized power grids. *Phys. Rev. Lett.*, 109:064101, Aug 2012.

[49] Andrej Vilfan and Frank Jülicher. Hydrodynamic flow patterns and synchronization of beating cilia. *Phys. Rev. Lett.*, 96:058102, Feb 2006.

[50] A. Puglisi and D. Villamaina. Irreversible effects of memory. *EPL (Europhysics Letters)*, 88(3):30004, nov 2009.

[51] Izrail Solomonovich Gradshteyn and Iosif Moiseevich Ryzhik. *Table of integrals, series, and products*. Academic press, 2014.

[52] Rouslan L Stratonovich. *Topics in the theory of random noise*, volume 2. CRC Press, 1967.

[53] Peter Reimann, Christian Van den Broeck, H Linke, Peter Hänggi, JM Rubi, and Agustın Pérez-Madrid. Giant acceleration of free diffusion by use of tilted periodic potentials. *Physical review letters*, 87(1):010602, 2001.

[54] M Büttiker, EP Harris, and R Landauer. Thermal activation in extremely underdamped josephson-junction circuits. *Physical Review B*, 28(3):1268, 1983.

[55] Hendrik Anthony Kramers. Brownian motion in a field of force and the diffusion model of chemical reactions. *Physica*, 7(4):284–304, 1940.

[56] Pascal Martin and AJ Hudspeth. Active hair-bundle movements can amplify a hair cell's response to oscillatory mechanical stimuli. *Proceedings of the National Academy of Sciences*, 96(25):14306–14311, 1999.

[57] Umberto Marini Bettolo Marconi, Andrea Puglisi, and Claudio Maggi. Heat, temperature and clausius inequality in a model for active brownian particles. *Scientific reports*, 7:46496, 2017.

[58] W Rüemelin. Numerical treatment of stochastic differential equations. *SIAM Journal on Numerical Analysis*, 19(3):604–613, 1982.

[59] Daniel T Gillespie. Exact numerical simulation of the ornstein-uhlenbeck process and its integral. *Physical review E*, 54(2):2084, 1996.

***

Appendix A

Functional Calculus

Consider a functional, $F[\psi]$, which maps from a vector space,V usually of continuous functions, $\psi : \Omega \to \mathbb{R}$, to real values $\mathbb{R}$. An important example of functional in physics is the action $S[q(t)]$, where the input is the trajectory(a function of time t, $q(t)$),

$$S[q(t)] = \int^t dt' L(\dot{q}(t), q(t), t) \tag{A.1}$$

Here I will discuss the simple calculus methods need for Functional analysis, mainly Functional derivative. Consider a functional,$F[\psi]$ which has values for $\psi(t)$ and $\psi(t) + \delta\psi_0(t)$ where $\delta\psi_0(t) \neq 0$ within $\tau - \delta t \leq t \leq \tau + \delta t$, then the functional derivative is then defined as

$$\frac{\delta F[\psi]}{\delta \psi(\tau)} = \lim_{\delta t \to 0} \frac{F[\psi + \psi_0] - F[\psi]}{\int_{\delta t} \delta\psi_0(t)dt} \tag{A.2}$$

Simplified way of looking at the above limit occurs when one consider the functional as a continuous limit of a multi-variable function. Assuming the analytic behaviour of the function, let the variable, $\psi(\tau)$ is perturbed slightly such that $\delta\psi_0(\tau) = \lambda\delta(t - \tau)$, then the above limit,we can redefine the above limit as

$$\frac{\delta F[\psi(t)]}{\delta \psi(\tau)} = \frac{dF[\psi(t) + \lambda\delta(t - \tau)]}{d\lambda}\bigg|_{\lambda=0} \tag{A.3}$$

Using the above definition, we can easily deduce the below results

$$(i) \quad F[\psi] = f(\psi(t)) \rightarrow \frac{\delta F[\psi(t)]}{\delta \psi(\tau)} = \frac{\partial f}{\partial \psi}\delta(t-\tau) \tag{A.4}$$

$$(ii) \quad F[\psi] = f(g(\psi)) \rightarrow \frac{\delta F[\psi(t)]}{\delta \psi(\tau)} = \frac{\partial f}{\partial g}\frac{\delta g}{\delta \psi(\tau)} \tag{A.5}$$

$$(iii) \quad F[\psi] = \int f(\psi,\dot{\psi})dt \rightarrow \frac{\delta F[\psi(t)]}{\delta \psi(\tau)} = \frac{\partial f}{\partial \psi(\tau)} - \frac{d}{d\tau}\frac{\partial f}{\partial \dot{\psi}} \tag{A.6}$$

Now, we can also extend the Novikov theorem, for multi-variable Gaussian random variable, to a functional,$g[\xi]$ of continuous stochastic process,$\xi(t)$ with i.i.d. Gaussian distribution, with first moment$\langle\xi(t)\rangle$ and second moment, $C(t,t') = \langle\xi(t)\xi(t')\rangle - \langle\xi(t)\rangle\langle\xi(t')\rangle$ is given by

$$\langle\xi(t)g[\xi]\rangle = \langle\xi(t)\rangle\langle g[\xi]\rangle + \int_0^t dt' C(t,t')\left\langle\frac{\delta g[\xi]}{\delta\xi(t')}\right\rangle \tag{A.7}$$

Appendix B

Numerical Recipe for stochastic dynamics

Numerical simulations provide a desk top method to model different system dynamics and stochastic differential equations describe the motion of particles under the effect of fluctuating environment. The key difference between numerical integration of deterministic equation of motion and SDE is that SDE requires different numerical schemes for better convergence based on the convention used to define SDE(mainly Ito or Stratonovich). Let us consider the SDE, given by

$$dx_t = a(x_t, t)dt + b(x_t, t) * dW_t \tag{B.1}$$

where dW_t is infinitesimal increment in Wiener process and $*$ is the notation for convention used to define SDE($'.'$ corresponds to Ito convention and $'\circ'$ corresponds to Stratonovich convention). Usually, dW_t is generated from psuedo-random generator for Gaussian distribution with 0 mean and variance dt.

The most basic integration scheme is called Euler-Mayurama method, where the next step is just dependent on the slope of the previous step. The scheme for the above SDE is given by

$$x_{t+\Delta t} = x_t + a(x_t, t)\Delta t + b(x_t, t) * \Delta W \tag{B.2}$$

where Δt is the time step and ΔW is the increment in the Wiener process obtained from $X \sim \mathcal{N}(0, \sqrt{\Delta t})$. This method has strong convergence for upto $O(\Delta t^{1/2})$ converges well to Ito convention for small Δt.

One can improve the above Euler's method by improving the estimate of the slope at the previous step for future prediction. The simplest improvement is called Heun's method or predictor-corrector method, where the slope for the next step is the average of slope at the previous step and the predicted step, given by

$$\tilde{x}_{t+\Delta t} = x_t + a(x_t, t)\Delta t + b(x_t, t)\Delta W \tag{B.3}$$

$$x_{t+\Delta t} = x_t + \frac{1}{2}\left[(a(x_t, t) + a(\tilde{x}_{t+\Delta t}, t + \Delta t)\Delta t + (b(x_t, t) + b(\tilde{x}_{t+\Delta t}, t + \Delta t)\Delta W\right] \tag{B.4}$$

This method has stronger convergence to Stratonovich convention and hence to have higher precision in the energetics(defined in the Stratonovich convention), one needs to use Heun's method or higher order Runge-Kutta method[58]

For a very few examples of SDE, one can find the exact solution to the differential equation and then we can directly work with the solution for the evaluation of the trajectories. For example, in the case of Ornstein-Ulhenbeck process, given by

$$dx_t = -kx_t dt + \sigma dW_t \tag{B.5}$$

where k and σ are constants.

In this case the exact updating formula[59] is given by

$$x_{t+\Delta t} = x_t \exp\left(-k\Delta t\right) + \left[\frac{\sigma}{2k}(1 - \exp(-2k\Delta t)\right]^{1/2} n \tag{B.6}$$

where n is taken from normal distribution, $X \sim \mathcal{N}(0, 1)$.

Appendix C

Chapman-Enskog Method for active bath

In this section, I will review a systematic expansion of the reduced equation for any driven system in an active bath case in the overdamped limit, extending a calculation done by Bonilla[39]. The method is based on perturbation method used to derive hydrodynamic equations from Boltzmann equation. Let us consider a Langevin dynamics of a driven particle in an active bath(OU process), where the equation of motion is given by

$$\dot{x}_t = f - \phi'(x_t) + \xi_t \quad ; \tau\dot{\xi}_t = -\xi_t + \sqrt{2D}\eta_t \tag{C.1}$$

where f, is he constant external driving force,$\phi(x)$ is the conservative potential and η_t is Gaussian white noise. Here we assumed the viscosity,γ, to be constant and taken to be unity(without loss of generality).

The adimensional form of Kramer's equation in the $(x, v = \dot{x})$ space with a constant external driving,f, according to the units in Table 3.1, is given by

$$\frac{\partial}{\partial v}\left[v + \frac{\partial}{\partial v}\right]P(x,v,t) = \epsilon\left[\frac{\partial P}{\partial t} + v\frac{\partial P}{\partial \theta} - \phi'\frac{\partial P}{\partial v} + f\frac{\partial P}{\partial v} - \epsilon\phi''\frac{\partial(vP)}{\partial v}\right] \tag{C.2}$$

where we have defined l to be the characteristic length of the system and the pertubative expansion is done on the parameter(assumed to be small) ,$\epsilon = \frac{\sqrt{D\tau}}{l} \ll 1$.

x	v	t	ϕ	f	P
l	$\sqrt{\frac{D}{\tau}}$	$l\sqrt{\frac{\tau}{D}}$	$D\gamma$	$\frac{D\gamma}{l}$	$\sqrt{\frac{\tau}{Dl^2}}$

Table C.1: Non-dimensionalizing units for Kramer's equation[]

The method of Champan-Enskog will be used to derive the equation for the marginal distribution, $R(x,t;\epsilon)$, for finite but small ϵ. Let us consider the full density to be written as :

$$P(x,v,t;\epsilon) = \frac{\exp(-v^2/2)}{\sqrt{2\pi}} R(x,t;\epsilon) + \sum_{j=1}^{\infty} \epsilon^j P^{(j)}(x,v;R) \tag{C.3}$$

$$\frac{\partial R}{\partial t} = \sum_{j=1}^{\infty} \epsilon^j \mathscr{F}^{(j)}(R) \tag{C.4}$$

The last equation is imposed based on the structure of the non-Markovian Master equation, which is the key ingredient of Chapman-Enskog method. Assuming the existence of solutions, one can obtain the functional, $\mathscr{F}^{(j)}(R)$, due to the structure of the adimensional Kramer's equation. One key observation, is that non-equilibrium steady state behaviour is not captured in the adminesional units, but one will retain it once we go back to the original dimensions. Integrating Eqn. (3.15) over v, we get

$$\frac{\partial R}{\partial t} + \frac{\partial J}{\partial x} = 0, \quad J(x,t;\epsilon) = \int vP(x,v,t;\epsilon)dv \tag{C.5}$$

From the above structure, we can also get

$$\mathscr{F}^{(j)}(R) = -\frac{\partial J^{(j)}}{\partial x}, \quad J^{(j)} = \int vP^{(j)}(x,v;R)dv \tag{C.6}$$

Putting Eqn.$(3.16-17)$ in Eqn. (3.15), we get a hierarchy of equations,

$$\mathscr{L}P^{(1)} \equiv \frac{\partial}{\partial v}\left(v + \frac{\partial}{\partial v}\right)P^{(1)} = v\frac{\exp[-v^2/2]}{\sqrt{2\pi}}\left(\phi'R - fR + \frac{\partial R}{\partial x}\right) \tag{C.7}$$

$$\mathscr{L}P^{(2)} = \frac{\exp[-v^2/2]}{\sqrt{2\pi}}[\mathscr{F}^{(1)} + (v^2-1)\phi''R] + v\frac{\partial P^{(1)}}{\partial x} + (f-\phi')\frac{\partial P^{(1)}}{\partial v} \tag{C.8}$$

$$\mathscr{L}P^{(3)} = v\frac{\partial P^{(2)}}{\partial x} + (f-\phi')\frac{\partial P^{(2)}}{\partial v} - \phi''\frac{\partial(vP^{(1)})}{\partial v} + \frac{\delta P^{(1)}}{\delta R}\mathscr{F}^{(1)}(R) \tag{C.9}$$

72

etc. The hierarchy of equations has similar structure to the one computed by Bonilla[]. Hence, the solutions of the equations also have same structure, product of polynomial in v and Gaussian in v, given by

$$P^{(2j+\varepsilon)}(x,v;R) = \frac{\exp[-v^2/2]}{\sqrt{2\pi}} \sum_{i=0}^{j} \mathscr{A}^{2j+\varepsilon}_{2i+\varepsilon} v^{2i+\varepsilon} \tag{C.10}$$

where $\varepsilon = 0, 1$. As the contributions from higher order terms become dominant, one would observe higher deviations from the Gaussian distribution in the velocity. One can easily deduce that $J^{(2j)} = 0$ and we have only odd orders of current. Solving the above hierarchy of equations we get

$$J^{(1)} = -\mathscr{D}R = -\left(\phi' - f + \frac{\partial}{\partial x}\right)R, \quad J^{(3)} = \frac{\partial}{\partial x}(\phi''R) \tag{C.11}$$

and the higher order currents as derived in [39], contains terms with 5th order derivative of the potential and the marginal distribution. But upto $O(\epsilon^5)$, we have

$$\frac{\partial R}{\partial t} = \epsilon\frac{\partial}{\partial x}\left(\phi'R - fR + \frac{\partial}{\partial x}[(1-\epsilon^2)R]\right) + O(\epsilon^5) \tag{C.12}$$

In the orginial units, upto $O(\tau^2)$, we get back the Sancho's approximation, given by

$$\frac{\partial R}{\partial t} = -\frac{\partial}{\partial x}[(f - \phi')R] + D\frac{\partial^2}{\partial x^2}[(1 - \tau\phi'')]R. \tag{C.13}$$